Journal of Medicinal Chemistry

Article

pubs.acs.org/jmc

Lead Optimization and Modulation of hERG Activity in a Series of Aminooxazoline Xanthene β-Site Amyloid Precursor Protein Cleaving Enzyme (BACE1) Inhibitors

Oleg Epstein,*[,†] Marian C. Bryan,[†,#] Alan C. Cheng,[§] Katayoun Derakhchan,[⊥] Thomas A. Dineen,[†] Dean Hickman,[∥] Zihao Hua,[†] Jason B. Human,[†] Charles Kreiman,[†] Isaac E. Marx,[†] Matthew M. Weiss,[†] Robert C. Wahl,[§] Paul H. Wen,[‡] Douglas A. Whittington,[§] Stephen Wood,[‡] Xiao Mei Zheng,[†] Robert T. Fremeau, Jr.,[‡] Ryan D. White,[†] and Vinod F. Patel[†,▽]

[†]Departments of Therapeutic Discovery, [‡]Neuroscience, [§]Molecular Structure and Characterization, [∥]Pharmacokinetics and Drug Metabolism, and [⊥]Comparative Biology and Safety Sciences, Amgen Inc., 360 Binney Street, Cambridge, Massachusetts 02142, One Amgen Center Drive, Thousand Oaks, California 91320, and 1120 Veterans Boulevard, South San Francisco, California 94080, United States

Supporting Information

ABSTRACT: The optimization of a series of aminooxazoline xanthene inhibitors of β-site amyloid precursor protein cleaving enzyme 1 (BACE1) is described. An early lead compound showed robust Aβ lowering activity in a rat pharmacodynamic model, but advancement was precluded by a low therapeutic window to QTc prolongation in cardiovascular models consistent with in vitro activity on the hERG ion channel. While the introduction of polar groups was effective in reducing hERG binding affinity, this came at the expense of higher than desired Pgp-mediated efflux. A balance of low Pgp efflux and hERG activity was achieved by lowering the polar surface area of the P3 substituent while retaining polarity in the P2′ side chain. The introduction of a fluorine in position 4 of the xanthene ring improved BACE1 potency (5−10-fold). The combination of these optimized fragments resulted in identification of compound **40**, which showed robust Aβ reduction in a rat pharmacodynamic model (78% Aβ reduction in CSF at 10 mg/kg po) and also showed acceptable cardiovascular safety in vivo.

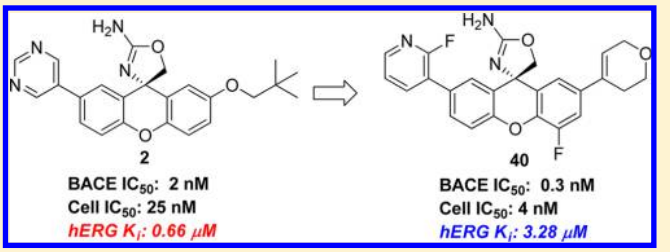

INTRODUCTION

Alzheimer's disease (AD) is a chronic and ultimately fatal neurodegenerative disease that directly or indirectly affects an increasing number of people.[1] AD represents a significant, unmet medical need worldwide as current treatments do not impact disease progression.[2] Although the cause of AD remains unclear, much evidence suggests that accumulation of β-amyloid (Aβ) peptides is a key contributor to disease progression.[3] In particular, human genetic evidence strongly implicates activating mutations that lead to increased Aβ production with early onset (familial) AD[4] while decreased Aβ production rate correlates with decreased incidence of neurodegeneration and AD.[5]

Leading approaches to develop a disease modifying treatment for AD have focused on the inhibition of Aβ production.[3] Aβ peptides arise from the amyloid precursor protein (APP) through two proteolytic steps, the first of which is mediated by the aspartyl protease β-site APP cleaving enzyme (BACE1).[6] Since BACE1 was characterized more than a decade ago, significant effort has been expended to identify orally available, small-molecule inhibitors that are able to effectively decrease Aβ production in the CNS of preclinical models. Unfortunately, early efforts focused on peptidomimetic inhibitors that failed to achieve meaningful target coverage in the CNS and/or adequate off-target selectivity.[7,8] More recent efforts have largely transitioned to scaffolds utilizing a cyclic amidine to engage the catalytic dyad that also have lower molecular weight with less conformational flexibility and increased success in avoiding efflux transporters (i.e., Pgp) to achieve acceptable exposure in the brain.[9,10] Importantly, multiple groups have reported robust lowering of Aβ in the CSF and brain in preclinical models as well as in humans with chemical matter from these scaffolds.[11,12]

We recently reported the discovery of aminooxazoline xanthenes as orally efficacious BACE1 inhibitors.[13] Initial optimization efforts demonstrated that the S2′ pocket of BACE1 enzyme could be exploited for improved potency and led to identification of compound **1**. This compound was a promising lead with good cellular potency combined with properties necessary for brain exposure. After brief exploration of close-in analogues, we found that homologation of the isobutyloxy P2′ substituent[14] to the larger neopentyloxy afforded compound **2** with improved potency and overall favorable properties where a significant pharmacodynamic (PD) effect in rats was observed (Table 1). A single oral dose (30 mg/kg)

Received: August 18, 2014

   dx.doi.org/10.1021/jm501266w | J. Med. Chem. XXXX, XXX, XXX−XXX

Table 1. In Vitro Profiles and PD Results for 1 and 2

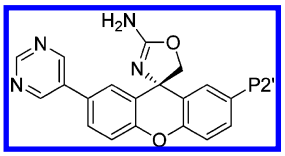

		BACE1 IC_{50} (nM)[a]					PD at 30 mg/kg, % Aβ reduction[f]	
compd	P_2'	enzyme	HEK[b]	hER[c]	hERG K_i (μM)[d]	HLM (μL/(min·mg))[e]	CSF	brain
1	OCH_2*i*-Pr	8 ± 0.3	36 ± 7	0.9	1.84	19	76	45
2	OCH_2*t*-Bu	2 ± 1	25 ± 8	1.5	0.66	21	80	61

[a]IC_{50} values were averaged values determined by at least two independent experiments. [b]Human embryonic kidney cells. [c]Efflux measured in LLC-PK1 cells transfected with human MDR1 and are reported as a ratio of (B to A)/(A to B). [d]From [^{3}H]-dofetilide binding assay. [e]Human liver microsomal (HLM) clearance. Compound concentration = 1 μM. Microsomal protein concentration = 250 μg/mL. [f]Pharmacodynamic assay measuring Aβ reduction in CSF and brain after 4 h postdose of test compound in naïve male Sprague−Dawley rats compared with vehicle treated animals.

Scheme 1. Preparation of Aminooxazoline Xanthenes 6a−f[a]

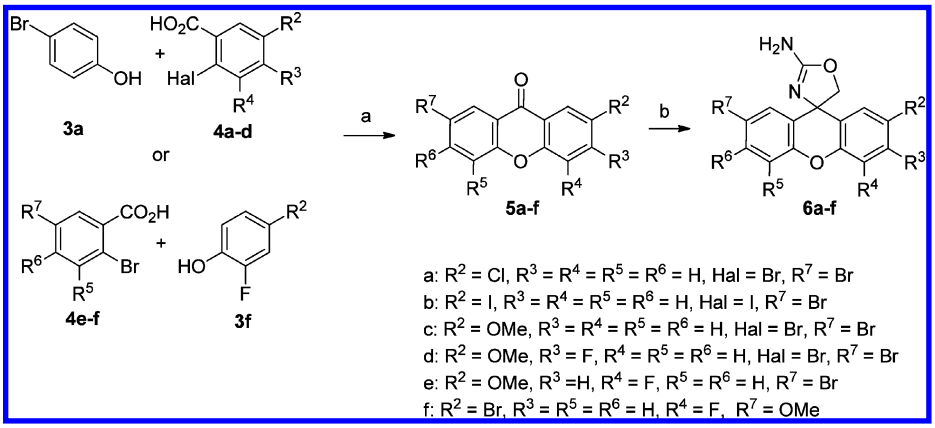

[a]Reagents: (a) (i) Cs_2CO_3, CuOTf (cat.), EtOAc (cat.), toluene, 90 °C, then HCl, (ii) H_2SO_4 or PPA, 60−110 °C, 26−85%; (b) (i) MeMgCl, THF, −10 °C, then PPTS or HCl, or $TMSCH_2Li$, THF, −78 °C, then AcCl, (ii) I_2, AgOCN, THF, 0 °C to rt, then NH_3, THF, 23−53%.

resulted in 61% brain Aβ reduction after 4 h. A dose response study from 0.3 to 30 mg/kg gave an $EC_{50,u}$ of 0.025 μM.[15] Unfortunately, the increased lipophilicity of **2** was associated with higher inhibitory activity of the hERG ion channel.[16] Assessment in an ex vivo isolated rabbit heart (IRH) model as well as an in vivo anesthetized dog model indicated an unacceptable margin for QTc prolongation that precluded further development of **2**.[17] Consequently, we sought to improve the cardiovascular (CV) safety profile in this series. Herein we describe the strategy and design considerations in our efforts to simultaneously minimize both hERG inhibition and efflux transporter recognition (i.e., Pgp) while maintaining BACE1 potency for robust CNS effect.

Avoiding inhibition of the hERG ion channel while simultaneously minimizing Pgp recognition and achieving potent BACE1 inhibition was considered a significant challenge given that the most straightforward strategies to address each parameter did not align toward a common physiochemical property profile. For example, reducing the basicity and overall lipophilicity of target molecules are common approaches for reducing hERG affinity.[18−20] However, for BACE1, it is known that decreasing basicity of the Asp-binding element typically decreases cellular BACE1 potency,[21−23] while introduction of polarity increases the total polar surface area (PSA), which is strongly correlated with increased Pgp recognition, leads to decreased exposure in the central compartment.[24] We sought to determine if it would be possible within the context of the xanthene series to balance hERG, Pgp efflux, and BACE1 potency by identifying regions of the molecule where polarity could be incorporated to minimize hERG activity without leading to significant efflux. The aminooxazoline warhead would initially be maintained (pK_a = 6.7)[25] and increased BACE1 potency explored by optimizing other key interactions observed in compound **2** while trying to limit further molecular weight increase in an already "large" core (~420 Da).

CHEMISTRY

For the preparation of aminooxazoline xanthenes, we followed our previously reported approach[13] depicted in Scheme 1. Suitably substituted phenols **3a,f** were arylated with 2-halobenzoic acids **4a−f** using Cu-catalyzed conditions reported by Buchwald and co-workers,[26] and the resulting 2-aryloxybenzoic acids underwent intramolecular Friedel−Crafts cyclization under acidic conditions to afford substituted xanthenones **5a−f**.[27] The carbonyl group was then converted to an exomethylene using MeMgCl followed by dehydration of the transient tertiary alcohol or through Peterson olefination by treatment with $TMSCH_2Li$ followed by acetyl chloride work-up.[28] Reaction of the olefin with iodine isocyanate generated from iodine and silver cyanate followed by treatment with ammonia afforded racemic aminooxazoline xanthenes **6a−f**.[29]

dx.doi.org/10.1021/jm501266w | J. Med. Chem. XXXX, XXX, XXX−XXX

Scheme 2. Preparation of Compounds 7, 8, 10, and 11[a]

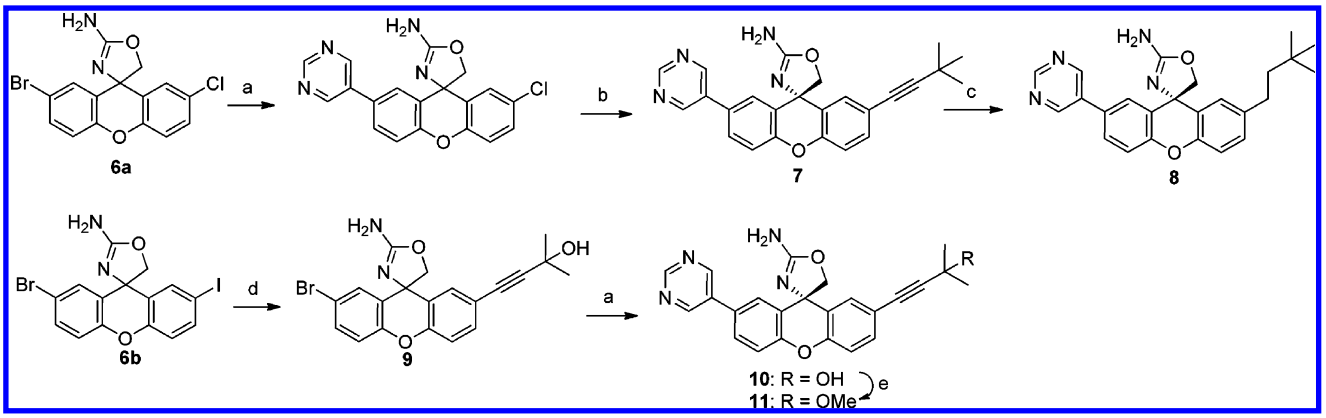

[a]Reagents: (a) 5-pyrimidylboronic acid, $Pd(PPh_3)_4$ (cat.), Na_2CO_3, dioxane/water, 22%; (b) (i) *t*-butylacetylene, $PdCl_2(PPh_3)_2$ (cat.), *t*-$Bu_3P{\cdot}HBF_4$, DBU, Cs_2CO_3, DMF, 150 °C, 49%, (ii) SFC separation; (c) H_2, Pd/C, 63%; (d) (i) 2-methyl-3-butyn-2-ol, $Pd(PPh_3)_4$ (cat.) CuI (cat.), *i*-$PrNH_2$, 97%, (ii) 5-pyrimidylboronic acid, $Pd(PPh_3)_4$ (cat.), Na_2CO_3, DME/water, 62%, (iii) SFC separation; (e) MsOH, MeOH, 35%.

Scheme 3. Preparation of Compounds 12−14[a]

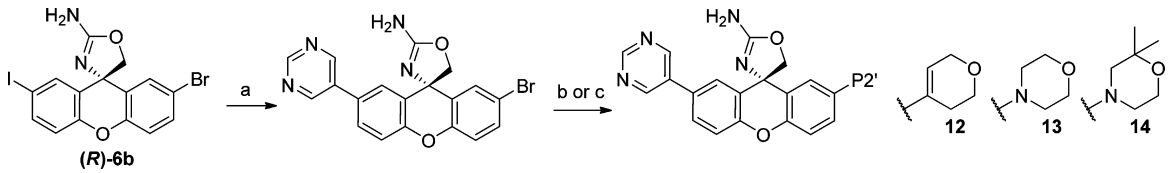

[a]Reagents: (a) 5-pyrimidylboronic acid, $Pd(PPh_3)_4$, Na_2CO_3, DMF/water, 62%; (b) 2-(3,6-dihydro-2*H*-pyran-4-yl)-4,4,5,5-tetramethyl-1,3,2-dioxaborolane, $Pd(Amphos)Cl_2$, K_2CO_3, dioxane/water, 65%; (c) morpholine or 2,2-dimethylmorpholine, X-Phos Palladacycle,[33] X-Phos, LiHMDS, THF, 17% for **13** and 19% for **14**.

Scheme 4. Preparation of O-Linked Compounds 16−21[a]

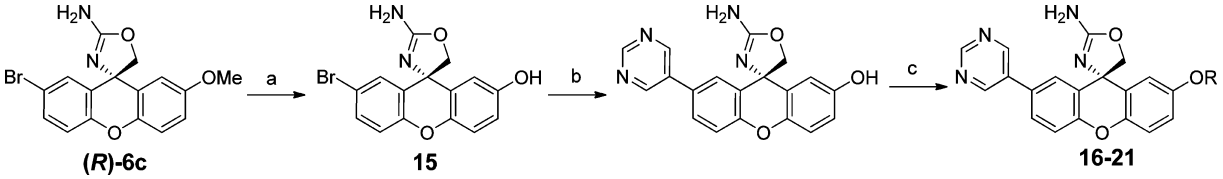

[a]Reagents: (a) BBr_3, DCM, 74%; (b) 5-pyrimidylboronic acid, $Pd(PPh_3)_4$, Na_2CO_3, DMF/water, 99%; (c) alkyl halide or alkyl triflate, Cs_2CO_3, DMF, 22−82%.

Initially, P3 and P2′ substituents were introduced into the racemic aminooxazoline core and enantiomerically pure final products were obtained after supercritical fluid chromatography (SFC) separation using a chiral stationary phase. For example, to prepare compound **7** which contained a *t*-butylacetylene P2′ group and 5-pyrimidinyl P3 group, the 2-chloro-7-bromo-derivative **6a** was used (Scheme 2). Selective Suzuki−Miyaura coupling[30] allowed the introduction of the P3 aryl substituents first, followed by installation of the P2′ alkyne moiety through a modified Sonogashira coupling.[31] The triple bond was then hydrogenated in the presence of palladium catalyst to afford **8** which contained a saturated alkyl P2′ substituent. The harsh conditions used for Sonogashira coupling of the aryl chlorides were not suitable for more sensitive alkynes such as propargylic alcohols, and the corresponding 2-iodo-7-bromo derivative **6b** was used instead for reversing the order of introduction of the P2′ and P3 substituents onto the xanthene core. Highly selective Sonogashira coupling of 2-iodo-7-bromo-substituted amino-oxazoline **6b** afforded aryl alkyne **9**. Suzuki coupling with 5-pyrimidylboronic acid followed by chiral SFC separation provided compound **10**. Treatment of the propargylic alcohol **10** with methanesulfonic acid in methanol afforded methoxy alkyne **11**.

2-Iodo-7-bromo aminoooxazoline xanthene **6b** was recognized as an exceptionally convenient template for the introduction of different substituents onto the xanthene core through selective palladium-catalyzed C−C and C−N coupling reactions. After chiral separation, both enantiomers of **6b** could be used for sequential installation of P2′ and P3 substituents. For example, compounds **12**, **13**, and **14** were prepared by selective Suzuki coupling of intermediate (*R*)-**6b** with 5-pyrimidyl boronic acid followed by another Suzuki coupling[32] with 4-dihydropyr-anyl boronate ester, resulting in **12** or Pd-catalyzed amination[33] to afford morpholines **13** and **14** (Scheme 3).

For the synthesis of oxygen-linked P2′ substituents, we primarily utilized the 7-bromo-2-methoxy substituted xanthene core (**6c**). Chiral separation of **6c** using SFC afforded enantiomerically pure (>99% ee) intermediate (*R*)-**6c**. Boron tribromide-mediated demethylation resulted in phenol **15** as a useful building block for further functionalization. Thus, introduction of 5-pyrimidyl P3 group followed by alkylation of

dx.doi.org/10.1021/jm501266w | J. Med. Chem. XXXX, XXX, XXX−XXX

the phenol represented a convenient way to efficiently prepare compounds with O-linked P2′ groups (**16**–**21**) (Scheme 4).

For screening of P3 substituents (compounds in Table 3), the neopentyloxy P2′ substituent was installed first and heteroaryl groups were introduced via Pd-catalyzed coupling of the aryl bromide **22** with commercially available boronic acids/boronate esters or organotin compounds to give **24**–**31** (Scheme 5). In

Scheme 5. Preparation of Compounds 24–32[a]

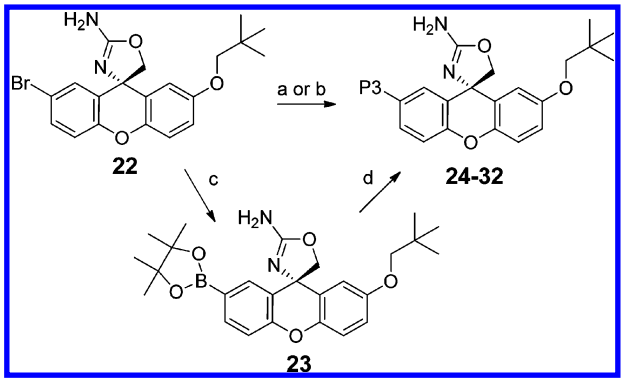

[a]Reagents: (a) P3-B(OH)$_2$, Pd(PPh$_3$)$_4$, Na$_2$CO$_3$, dioxane/water, 6–77%; (b) 2-(tributylstannyl)pyridine, Pd(PPh$_3$)$_4$, DMF, 24%; (c) B$_2$Pin$_2$, Pd(dppf)Cl$_2$, KOAc, dioxane; (d) 2,4-difluoro-3-iodopyridine, Pd(Amphos)Cl$_2$, KOAc, BuOH/water, 53%.

cases when heteroaryl halides were commercially available, aminooxazoline intermediate **22** was converted to boronic ester **23**, which was used in Suzuki coupling reactions to prepare compound **32** (Table 3).

Preparation of the BACE1 inhibitors included in Table 4 was achieved by similar methods using fluorinated aminooxazoline xanthenes **6c**–**e** as described in Scheme 4 through sequential introduction of heteroaryl P3 substituents via Suzuki coupling followed by alkylation of the corresponding phenols with 3-(bromomethyl)-3-methyloxetane.

The preparation of 4-fluoro-substituted aminooxazoline xanthenes **37**–**44** (Table 5) was streamlined using a single intermediate (*S*)-**6e**. As described in Scheme 6, demethylation of bromomethoxy derivative (*S*)-**6e** followed by Suzuki coupling of the phenol **45** with 2-fluoro-3-pyridylboronic acid gave **46**. Phenol **46** could be alkylated to afford alkoxy-substituted compounds **37** and **38**. Activation of the phenol was achieved through aryl triflate formation, and the triflate **47** was subsequently used in Pd-catalyzed C–C and C–N coupling reactions to install a variety of P2′ groups.

RESULTS AND DISCUSSION

We began optimization by exploring S2′pocket while maintaining the P3[14] pyrimidyl substituent (Table 2). As expected, introduction of lipophilic groups resulted in compounds with a significant increase in hERG inhibitory activity, especially when cLogP >3.5, (compounds **7**, **8**, and **16**, Table 2). Introduction of polarity into the P2′ group to afford compounds with cLogP in a lower range (1.7–3) gave more promising results. For example, introduction of a polar hydroxyl group (**10** and **17**) significantly reduced hERG inhibitory activity compared to compound **2** but at the expense of high Pgp-mediated efflux, likely due to the presence of an additional hydrogen bond donor. Substitution to a cyano group or oxetane (**20** and **21**) also led to compounds which demonstrated high efflux, presumably a result of increased total PSA. Incorporating a fluorine atom into the P2′ group (**19**) lowered hERG activity to 5 μM with only a minor effect on Pgp efflux. Masking PSA from Pgp recognition by the addition of neighboring lipophilic groups was effective in lowering efflux but overall led to increased microsomal turnover consistent with the increase in cLogP (cf. **10** and **11**, **17** and **18**, **13** and **14**). A desirable combination of BACE1 potency, balanced with low hERG activity (>10 μM) and a relatively low efflux ratio, was found in compound **12**, containing a 4-dihydropyranyl P2′ substituent.

With the initial goal of changing the distribution of PSA around the molecule as a means of potentially better separating BACE1 potency from hERG and Pgp efflux, we performed an additional screen of P3 groups while keeping the neopentyloxy P2′group constant. As can be seen from selected data shown in Table 3, the position of the nitrogen atom in the P3 substituent is important for maintaining high BACE1 enzymatic activity (3-pyridinyl (**26**), being superior to 2- and 4-pyridinyl (**24** and **25**)). Fluorine substitution was well tolerated around 3-pyridyl ring (**27**, **29**, **31**, and **32**). Substitution at the 3-position of the pyridine ring was well tolerated (**28**–**30**), although introduction

Scheme 6. Preparation of 4-Fluoro-Substituted Aminooxazoline Xanthenes 37–44[a]

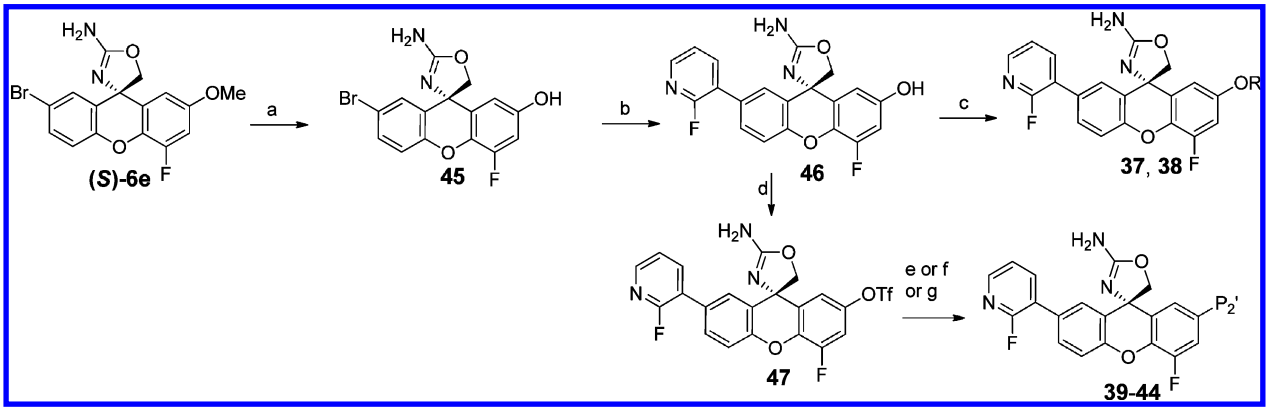

[a]Reagents: (a) BBr$_3$, DCM, 96%; (b) 2-fluoro-3-pyridylboronic acid, Pd(PPh$_3$)$_4$, Na$_2$CO$_3$, DMF/water, 87%; (c) 3-(bromomethyl)-3-methyloxetane or 2-fluoro-2-methylpropyl trifluoromethanesulfonate, Cs$_2$CO$_3$, NaI, DMF, 35% for **37** and 60% for **38**; (d) *N*-(5-chloro-2-pyridyl)bis-(trifluoromethanesulfonimide) (Commins' reagent), Et$_3$N, DCM, 84%; (e) RB(OH)$_2$, Pd(PPh$_3$)$_4$, Na$_2$CO$_3$, dioxane/water; (f) amine, Pd$_2$dba$_3$, DavePhos, LiHMDS, THF, 11–61%; (g) 2-pyridylzinc chloride, Pd(PPh$_3$)$_4$, THF, 72%.

dx.doi.org/10.1021/jm501266w | J. Med. Chem. XXXX, XXX, XXX–XXX

Table 2. Selected SAR of P2′ Substituents

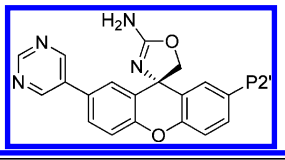

Compd	P2'	BACE1 IC_{50}, nM[a] Enzyme	HEK[b]	Average P_{app}[c] (10^{-6} cm/s)	hER[d]	hERG K_i[f] (μM)	HLM[e] (μL/(min·mg))	cLogP	PSA (sq. Å)
2	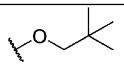	2±1	25±8	13.6	1.6	0.66	21	3.76	92
7	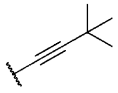	3.1±1.5	36±8	12.7	1.0	0.15	17	4.11	83
8	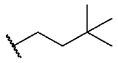	2±1	49±23	6.8	1	0.41	69	4.87	83
10	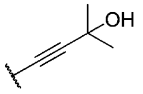	7±	20±0.3	10.9	16.9	14	<14	1.50	103
11	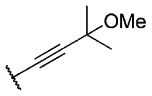	4±0.4	19±2	13.2	1.1	1.42	160	2.22	92
12	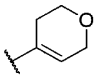	6±1	16±2	13.5	2.6	10.7	72	2.10	92
13	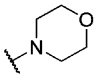	17±1	48±16	14.3	13.8	>15	21	1.44	95
14	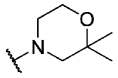	11±1	30±7	13.2	3.7	>15	73	2.47	95
16	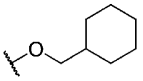	7±0.4	269±7	2.4	1.1	0.09	129	4.55	92
17	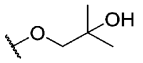	7±0.6	15±0.7	12.4	41.5	>15	<14	1.74	112
18	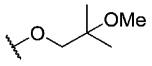	4±0.5	10±6	17.4	3.6	>15	74	2.50	101
19	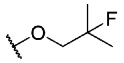	8±2	30±10	14.8	2.3	4.98	<14	3.08	92
20	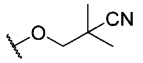	9±3	21±2	22.3	9.1	11.70	<14	2.01	116
21	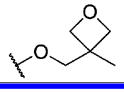	7±2	10±3	20.7	15.7	>15	40	2.26	101

[a]IC_{50} values were averaged values determined by at least two independent experiments. [b]Human embryonic kidney cells. [c]Apparent permeability measured in parental LLC-PK1 cells. Values are an average of apical to basolateral (A to B) and basolateral to apical (B to A) velocities and are reported as 10^{-6} cm/s. [d]Efflux measured in LLC-PK1 cells transfected with human MDR1 and are reported as a ratio of (B to A)/(A to B). [e]Human liver microsomal (HLM) clearance. Compound concentration = 1 μM. Microsomal protein concentration = 250 μg/mL. [f]From [^{3}H]-dofetilide binding assay.

of a methoxy group in **30** led to poor metabolic stability. Out of this set of P3 groups, 2-fluoro-3-pyridinyl and 2,4-difluoropyridinyl substituents led to increased BACE1 inhibition. Moreover, the two compounds containing these P3 groups (**31** and **32**) did not show significant hERG inhibition despite cLogP values ∼5. This suggests that overall lipophilicity of the molecules is not solely responsible for activity on hERG channel, and subtle structural modifications could disrupt interactions that affect hERG affinity. Considering potential complications arising from chemical reactivity of the 2-fluoro-substituted pyridine moiety, compounds containing these groups were incubated in buffered solutions in the presence of glutathione (GSH), as well as with hepatocytes, and only the compounds with 2,4-difluoro-3-pyridine group showed formation of a GSH-conjugate (data not shown). On the basis of these findings and overall profile of compounds with the 2-fluoro-3-pyridinyl group, this P3 group was preferred for further optimization in this series.

Changing focus from decreasing hERG activity to improving BACE1 potency, we carefully examined a crystal structure of **2** with BACE1 (Figure 1). This cocrystal suggested that

dx.doi.org/10.1021/jm501266w | J. Med. Chem. XXXX, XXX, XXX−XXX

Table 3. Selected SAR of P3 Substituents

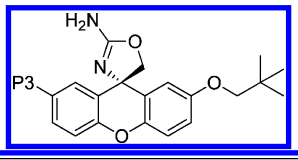

Compd	P3	BACE1 IC_{50} (nM)[a] Enzyme	BACE1 IC_{50} (nM)[a] HEK[b]	hER[d]	hERG K_i[f] (μM)	HLM (μL/(min·mg))[e]	cLogP	PSA (sq. Å)
2	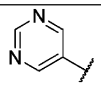	2±1	25±8	1.6	0.661	21	3.75	92
24		23±2	583±7	1	0.496	51	4.92	79
25		323±71	2,830±30	1.1	0.624	25	4.71	79
26		4±0.2	74±20	1.1	0.797	36	4.71	79
27	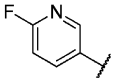	6±1	113±3	1	0.259	23	4.94	79
28	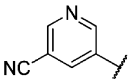	3±0.9	40±3	1	0.145	87	4.34	103
29	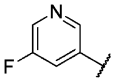	4±1	76±25	1	0.377	34	4.94	79
30	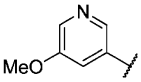	4±0.01	80±11	1	>15	116	5.13	88
31		0.8±0.02	39±14	1	>15	24	4.94	79
32	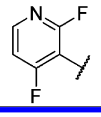	0.5±0.03	45±3	1.7	>15	22	5.11	79

[a]IC_{50} values were averaged values determined by at least two independent experiments. [b]Human embryonic kidney cells. [c]Apparent permeability measured in parental LLC-PK1 cells. Values are an average of apical to basolateral (A to B) and basolateral to apical (B to A) velocities and are reported as 10^{-6} cm/s. [d]Efflux measured in LLC-PK1 cells transfected with either rat MDR1A/1B or human MDR1 and are reported as a ratio of (B to A)/(A to B). [e]Human liver microsomal (HLM) clearance. Compound concentration = 1 μM. Microsomal protein concentration = 250 μg/mL. [f]From [^{3}H]-dofetilide binding assay.

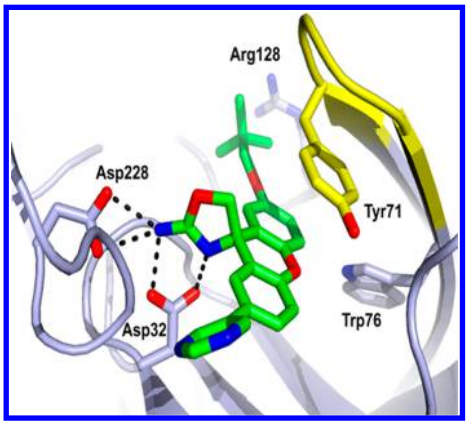

Figure 1. Crystal structure of compound **2** in complex with BACE1.

introducing substituents in the xanthene core may result in additional favorable interactions. Particularly intriguing was the potential to interact with Trp 76 via positions 3 and/or 4 of the xanthene ring. We hypothesized that a heteroatom (N or F) at either of these positions could lead to a beneficial interaction with the protein to improve binding affinity.[34] Similar interactions of fluorine, oxygen, and nitrogen atoms with the NH of Trp76 in crystal structures of inhibitors with the BACE1 protein have been reported to lead to increased BACE1 potency.[18,22,35,36]

To explore this possibility, we initially examined fluorination at different positions of the xanthene ring in combination with preferred P3 and P2′ groups. Selected results of the initial screen are shown in Table 4. Introduction of a fluorine atom at the 3 position led to marginal improvements of both enzyme and cell potency compared to the unsubstituted core. A fluorine atom at the 4 position resulted in a 7-fold improvement in enzymatic potency and a ∼4-fold improvement in cellular activity. Fluorine

dx.doi.org/10.1021/jm501266w | J. Med. Chem. XXXX, XXX, XXX−XXX

Table 4. Screen of F-Substitution on the Xanthenes Ring

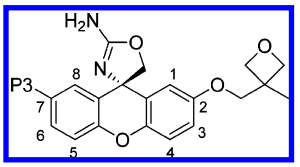

			BACE1 IC_{50} (nM)[a]					metabolic stability (μL/(min·mg))[e]	
compd	xanthene core	P3	enzyme	HEK[b]	P_{app} (10^{-6} cm/s)[c]	hER[d]	rER[d]	RLM	HLM
33	all-H	3-Py	7 ± 2	15 ± 2	8.8	4.1	5.1	67	47
34	3-F	3-Py	4 ± 0.8	12 ± 7	13.5	1.4	2.9	67	91
35	4-F	3-Py	1 ± 0.08	4 ± 0.3	15.2	2	3.3	67	129
36	5-F	3-Py	71 ± 15	178 ± 6	7.1	5.2	6.3	71	82
37	4-F	2-F-3-Py	0.4 ± 0.1	3 ± 1	12.7	1.3	1.8	40	108

[a]IC_{50} values were averaged values determined by at least two independent experiments. [b]Human embryonic kidney cells. [c]Apparent permeability measured in parental LLC-PK1 cells. Values are an average of apical to basolateral (A to B) and basolateral to apical (B to A) velocities and are reported as 10^{-6} cm/s. [d]Efflux measured in LLC-PK1 cells transfected with either rat MDR1A/1B or human MDR1 and are reported as a ratio of (B to A)/(A to B). [e]Rat liver microsomal (RLM) and human liver microsomal (HLM) clearance. Compound concentration = 1 μM. Microsomal protein concentration = μg/mL.

substitution at the 5-position was not well tolerated, with a ∼10-fold drop in BACE1 activity. As previously observed in our P3 group screen, the 2-fluoro-3-pyridyl P3 group was superior to 3-pyridyl and brought additional potency in the enzymatic and cellular assays (**37**).

As a next step, we combined our findings from the xanthene core substitution (4-fluoro-) and P3 group (2-fluoro-3-pyridyl) and performed an additional screen of P2′ substituents including groups that were identified in our initial optimization to lower the hERG affinity of pyrimidine P3 derivatives (Table 5). We were pleased to find that the previously described SAR translated well to the 4-F xanthenes, affording compounds with favorable in vitro properties. Compounds from this series showed single-digit nanomolar BACE1 inhibitory activity in the cellular assay and permeability and efflux properties expected to allow for CNS exposure. Notably, the 3-dihydropyranyl P2′ group provided the same level of BACE1 activity as the 4-dihydropyranyl isomer (**39** and **40**, respectively) although with elevated liver microsomal turnover, while morpholine **41** and 3-fluoro-substituted pyrrolidine **42** were also well tolerated. Selected 5- and 6-membered ring heterocyles (**43** and **44**) also represent suitable P2′ substitution, resulting in compounds with low hERG inhibition and desirable in vitro profiles.

In vivo reduction of Aβ levels was initially examined using naïve Sprague–Dawley (SD) rats that were dosed orally at 10 mg/kg. After a single dose, compound plasma exposure and Aβ levels (both CSF and brain) were measured at the 4 h time point. Significant inhibition of Aβ production was observed for most of the compounds with high BACE1 cellular potency and good microsomal stability. Despite favorable in vitro properties, low PD response was observed for oxetane-containing compound **37** as a result of poor in vivo target coverage (exposure multiple $C_{plasma,u}$/cell IC_{50} = 0.5). Compounds were rank ordered using estimates from single-point experiment unbound plasma concentrations to achieve 50% Aβ lowering in brain.[37] In general, compounds with low efflux showed little shift between the cellular IC_{50} and in vivo PD EC_{50} determined from a time-course experiment or estimated from the single-point screen. Compound **40** showed a very robust in vivo PD response at 10 mg/kg dose (78% in CSF and 67% in brain). The unbound plasma EC_{50} for brain effect of **40** in this single dose PD experiment was 13 nM. Given the small difference between PD EC_{50} and cellular IC_{50} (4 nM), minimal impairment at the blood–brain barrier due to Pgp efflux was observed and consistent with low measured Pgp efflux.[38]

The crystal structure of compound **40** bound to BACE1 was refined to 1.78 Å (Figure 2). As seen in previous structures of aminooxazoline xanthene compounds, the amidine moiety interacts with the two catalytic aspartic acids and Tyr71 engages in a π-stacking interaction with the xanthene core. As anticipated, the fluorine atom in position 4 of the xanthene ring interacts with Trp76 via a hydrogen bond,[39] likely the reason for the increased BACE1 inhibitory activity. The fluoropyridine side chain occupies the S3 pocket of BACE1, with the nitrogen atom involved in a water-mediated H-bonding interaction with the backbone carbonyl of Ser229, and the dihydropyran unit resides in the S2′ pocket of the protein where the oxygen atom is within hydrogen bond distance to Arg128.

Compound **40** was evaluated further in both time-course and dose–response rat PD model studies. Pharmacodynamic studies in rats at oral doses of 1, 3, 10, and 30 mg/kg showed dose-and exposure-dependent reduction of Aβ level at the 4 h time point. Unbound plasma concentrations to achieve 50% Aβ reduction were determined to be 0.005 and 0.010 μM for CSF and brain effects, respectively (Figure 3).

Time-dependent reduction of Aβ with compound **40** was also studied at a 30 mg/kg dose using 1.5, 4, 7, 10, 16, and 24 h time points. Maximum Aβ lowering in both the brain and CSF was observed between 4 and 10 h (Figures 4 and 5), with levels returning to baseline after 24 h. Pharmacokinetic/pharmacodynamic (PK/PD) modeling of **40** using an indirect response model that accounts for the formation and clearance of Aβ in CSF[40] estimated the in vivo plasma $IC_{50,\ unbound}$ for CSF and brain effects of **40** to be 0.017 and 0.013 μM, respectively.

Importantly, the QT prolongation issues associated with **2** were not observed with **40**. Although the in vitro margin between hERG inhibition (3.28 μM) and BACE1 cell IC_{50} (4 nM) for **40** was large (820-fold), the compound was assessed further in ex vivo and in vivo CV safety models. In the ex vivo IRH model, hearts (n = 3) were perfused with five concentrations of **40** at increasing doses of 0.1, 0.3, 1, 3, and 10 μM. Each dose was applied for 20 min with measurements collected continuously. No effect on QTc interval was observed at any of the doses. In an anesthetized dog CV model, anesthetized dogs (n = 2) were

dx.doi.org/10.1021/jm501266w | J. Med. Chem. XXXX, XXX, XXX–XXX

Table 5. Selected SAR of 4-Fluoro Xanthene Series

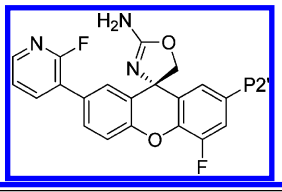

Compd	P2'	BACE1 IC_{50} (nM)[a] HEK[b]	P_{app} (10^{-6}cm/s)[c]	hER[d]	rER[d]	hERG K_i (μM)[e]	Metabolic stability ((μL/min)/mg)[f] RLM	HLM	PD response at 10 mg/kg, % Aβ reduction[g] CSF	brain	PD $EC_{50\,u}$ brain effect, nM[h]
37	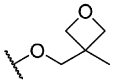	3±1	12.7	1.3	1.8	>15	40	108	18	13	NC
38	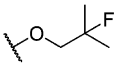	9±6	9.8	1	1	>15	<14	<14	73	62	25
39		3±0.6	17.6	1.2	1.2	>15	79	75	74	51	8
40		4±1	6.9	1	1	3.28	27	46	78	67	13
41		5±1	17.8	1.6	2.5	>15	28	27	74	64	86
42	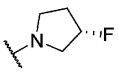	7±2	9.8	1.6	1.7	>15	32	82	62	45	59
43		3±0.2	13	1.1	2.1	>15	<14	<14	74	64	366
44	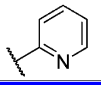	12±3	14.4	1	1.3	2.77	<14	<14	66	61	58

[a]IC_{50} values were averaged values determined by at least two independent experiments. [b]Human embryonic kidney cells. [c]Apparent permeability measured in parental LLC-PK1 cells. Values are an average of apical to basolateral (A to B) and basolateral to apical (B to A) velocities and are reported as 10^{-6} cm/s. [d]Efflux measured in LLC-PK1 cells transfected with either rat MDR1A/1B or human MDR1 and are reported as a ratio of (B to A)/(A to B). [e]From [^{3}H]-dofetilide binding assay. [f]Rat liver microsomal (RLM) and human liver microsomal (HLM) clearance. Compound concentration = 1 μM. Microsomal protein concentration = 250 μg/mL. [g]Pharmacodynamic assay measuring Aβ reduction in CSF and brain after 4 h postdose of test compound in naïve male Sprague−Dawley rats comparing with vehicle treated animals. [h]Estimated unbound plasma EC_{50} for brain effect from a single dose experiment at 4 h time point.

treated intravenously with 30 min infusions of **40** at doses of 3.3, 11, and 35 mg/kg. Average unbound plasma concentrations of 0.049, 0.356, and 0.654 μM were achieved where only 11% increase in QTc interval in one subject was observed at the highest dose, affording a 65-fold margin over the plasma $EC_{50,unbound}$ for brain Aβ reduction in rats and a 50-fold margin over the in vivo $IC_{50,unbound}$ as determined by the indirect response model.

CONCLUSION

In conclusion, optimization of a series of aminooxazoline xanthenes was performed with an emphasis on mitigating the hERG-mediated QTc prolongation observed in an anesthetized dog CV safety model. It was determined that introduction of polarity in the P2′ region of the inhibitor while simultaneously removing polarity from P3 enabled the identification of inhibitors with lower hERG binding affinity without sacrificing brain exposure and metabolic stability. Introduction of a fluorine in the 4-position of the xanthene ring increased BACE1 enzyme and cellular potency resulting in compounds that produced robust reductions in CSF and brain Aβ levels in a naïve rat pharmacodynamic model. Compound **40** was selected for further advancement based on its excellent in vitro profile and in vivo PD response. Profiling of this compound in a dog cardiovascular safety model showed significant improvement to **2** with only minor effects on the QTc interval at exposures approximately 50-fold over the in vivo $IC_{50,unbound}$.

EXPERIMENTAL SECTION

Chemistry. Unless otherwise noted, all materials were obtained from commercial suppliers and used without further purification. Anhydrous solvents were obtained from Aldrich or EM Science and used directly.

dx.doi.org/10.1021/jm501266w | J. Med. Chem. XXXX, XXX, XXX−XXX

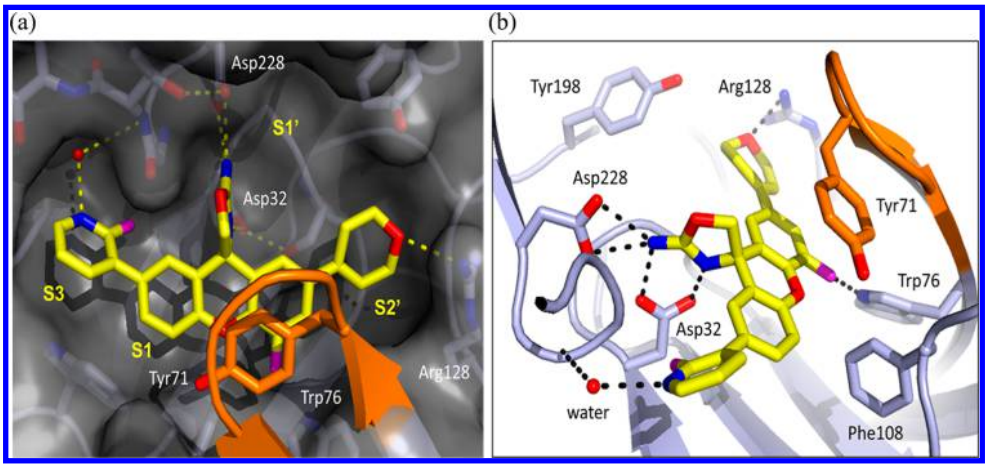

Figure 2. Cocrystal structure of **40** with BACE1. (a) Interactions of **40** with the catalytic aspartic acids of BACE1. (b) Interactions of fluorine atom with Trp76 and the dihydropyran moiety with Arg128 in P2′.

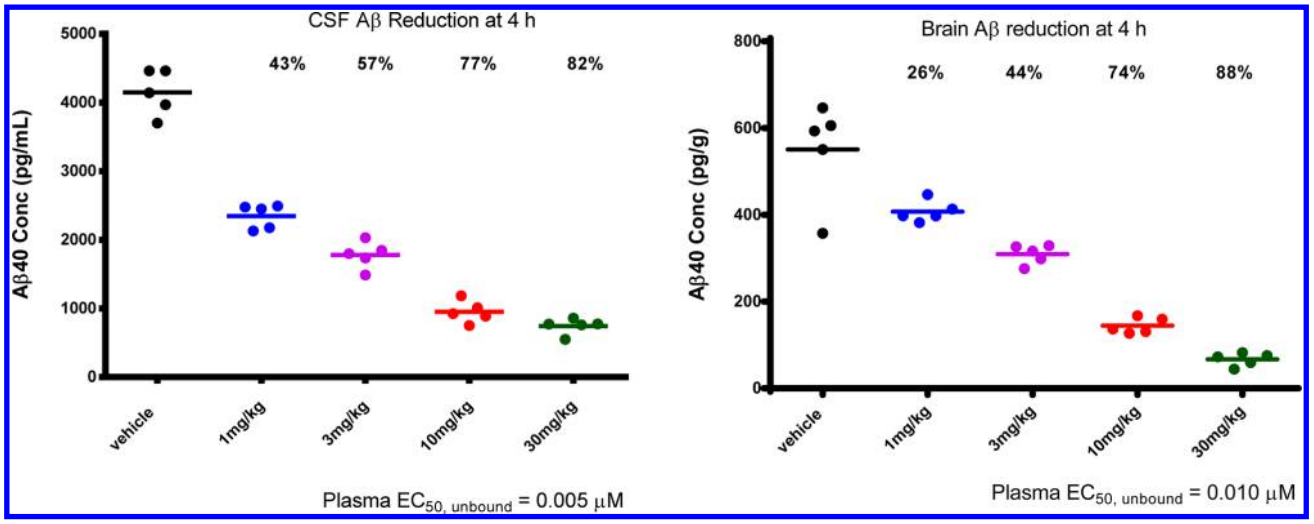

Figure 3. Dose dependent reduction of Aβ in a rat pharmacodynamic model at 4 h after oral dose of **40**.

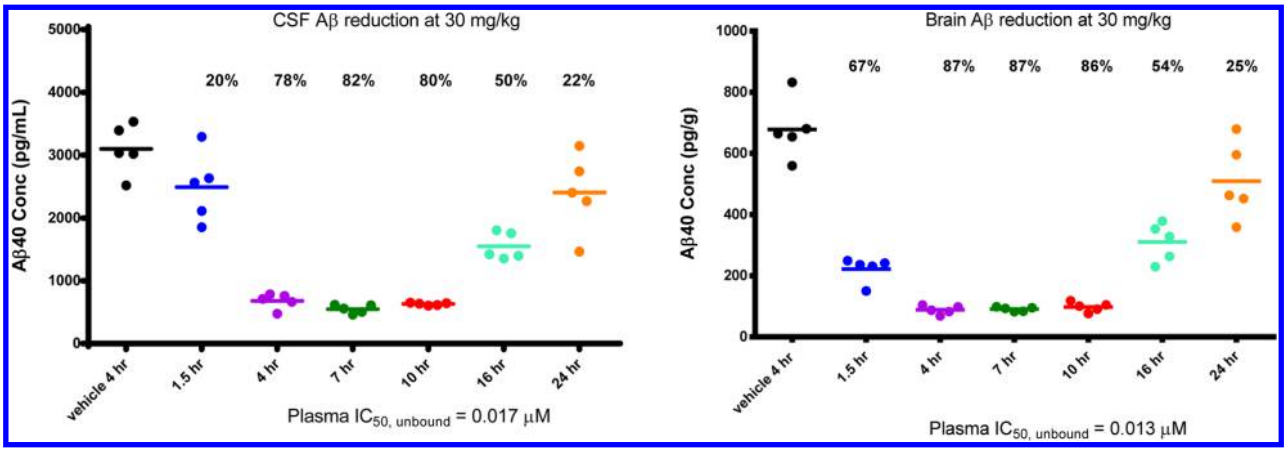

Figure 4. Time dependent reduction of Aβ in rat pharmacodynamic model after 30 mg/kg oral dose of **40**.

All reactions involving air- or moisture-sensitive reagents were performed under a nitrogen or argon atmosphere. All microwave assisted reactions were conducted with a Smith synthesizer from Personal Chemistry, Uppsala, Sweden. Silica gel chromatography was performed using prepacked silica gel cartridges (Biotage or ISCO). ^{1}H NMR spectra were recorded on a Bruker AV-400 (400 MHz) spectrometer at ambient temperature. Chemical shifts are reported in parts per million (ppm, δ units) downfield from tetramethylsilane. Data are reported as follows: chemical shift, multiplicity (s = singlet, d = doublet, t = triplet, q = quartet, dd = double of doublets, dt doublet of triplets, etc., br = broad, m = multiplet), coupling constant(s), and number of protons. Purity for final compounds was greater than 95% unless otherwise noted and was measured using Agilent 1100 series high performance liquid chromatography (HPLC) systems with UV

dx.doi.org/10.1021/jm501266w | J. Med. Chem. XXXX, XXX, XXX−XXX

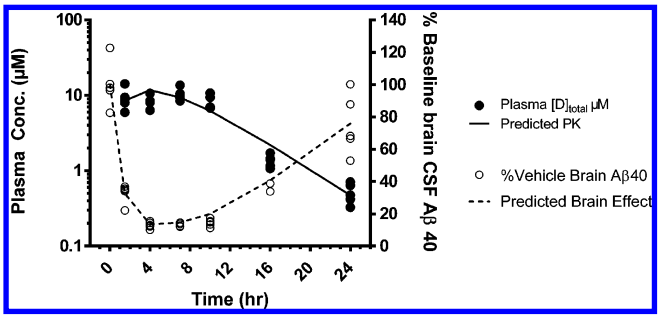

Figure 5. Reduction of brain Aβ levels in rats after 30 mg/kg oral dose of **40**.

detection at 254 nm (system A, Agilent Zorbax Eclipse XDB-C8 4.6 mm × 150 mm, 5 μm, 5−100% CH_3CN in H_2O with 0.1% TFA for 15 min at 1.5 mL/min; system B, Waters Xterra 4.6 mm × 150 mm, 3.5 μm, 5−95% CH_3CN in H_2O with 0.1% TFA for 15 min at 1.0 mL/min).

*7-Bromo-4-fluoro-2-methoxy-9H-xanthen-9-one (**5e**).* Step 1: A 5 L round-bottom flask equipped with a reflux condenser and overhead stirrer was charged with 2-fluoro-4-methoxyphenol (140 g, 982 mmol), 2,5-dibromobenzoic acid (250 g, 893 mmol), ethyl acetate (4.4 mL, 44.7 mmol), and toluene (2500 mL). Copper(I) triflate toluene complex (2:1) (4.75 g, 22.3 mmol) was added, and then cesium carbonate (582 g, 1786 mmol) was carefully added in portions. The mixture was stirred for 10 min at room temperature then heated at 95 °C for 3 h. The toluene was distilled off under vacuum. The residue was dissolved in 2 L of water and washed with 500 mL of EtOAc. The aqueous layer was acidified with concentrated HCl to pH 2, and the precipitate was collected by filtration and washed with water two times and dried on air. The resulting solid was washed with a 4:1 hexane/ethyl acetate twice and then dried under vacuum to afford 5-bromo-2-(2-fluoro-4-methoxyphenoxy)benzoic acid (235 g, 689 mmol, 77% yield) as a brown solid. ^{1}H NMR (400 MHz, DMSO-d_6) δ ppm 13.24 (br s, 1 H), 7.89 (d, J = 2.5 Hz, 1 H), 7.65 (dd, J = 8.9, 2.5 Hz, 1 H), 7.08−7.16 (m, 1 H), 7.04 (dd, J = 12.7, 2.9 Hz, 1 H), 6.80 (ddd, J = 9.0, 2.9, 1.4 Hz, 1 H), 6.75 (dd, J = 9.0, 0.6 Hz, 1 H), 3.78 (s, 3H). MS m/z = 341.0 $[M + H]^+$.

Step 2: To polyphosphoric acid (1130 g, 1150 mmol) in a 2 L round-bottom flask equipped with an overhead stirrer was added crude 5-bromo-2-(2-fluoro-4-methoxyphenoxy)benzoic acid (197 g, 577 mmol) from the previous step, and the viscous mixture was stirred at 125 °C for 2 h. The viscous solution was cooled slightly and poured into well stirred (overhead stirrer) ice−water (3 L). After 45 min of stirring, the solids were collected by filtration on a glass filter and washed sequentially with water, 1N NaOH, and then twice with water. The filter cake was dried for 18 h on the filter under vacuum, and the solids were then further dried by azeotroping with toluene to afford 7-bromo-4-fluoro-2-methoxy-9*H*-xanthen-9-one (**5e**) (160 g, 495 mmol, 86% yield) as an off-white solid. ^{1}H NMR (400 MHz, DMSO-d_6) δ ppm 8.25 (d, J = 2.6 Hz, 1 H), 8.04 (dd, J = 9.0, 2.6 Hz, 1 H), 7.73 (d, J = 9.0 Hz, 1 H), 7.61 (dd, J = 12.3, 3.0 Hz, 1 H), 7.38 (dd, J = 3.0, 1.6 Hz, 1 H), 3.89 (s, 3 H). MS m/z = 323.0 $[M + H]^+$.

*(S)-7′-Bromo-4′-fluoro-2′-methoxy-5H-spiro[oxazole-4,9′-xanthen]-2-amine ((S)-**6e**).* Step 1: 7-Bromo-4-fluoro-2-methoxy-9*H*-xanthen-9-one (39.5 g, 122 mmol) was dissolved in 580 mL of THF and cooled to −30 °C in a dry ice acetonitrile bath. Methylmagnesium chloride (3 M in THF) (82 mL, 245 mmol) was added via addition funnel over 30 min while maintaining temp < −15 °C. After 1 h, the mixture was allowed to warm to 0 °C. The mixture became homogeneous after 2.5 h. The reaction was carefully quenched with saturated NH_4Cl (100 mL) and diluted with brine (200 mL). The aqueous layer was extracted with ethyl acetate, and the combined organic layers were washed with brine and dried over anhydrous sodium sulfate. Concentration of the mixture in vacuo afforded crude 7-bromo-4-fluoro-2-methoxy-9-methyl-9*H*-xanthen-9-ol (42.0 g) as a tan semi-solid and was advanced without further purification.

Step 2: To a 1 L round-bottom flask charged with 7-bromo-4-fluoro-2-methoxy-9-methyl-9*H*-xanthen-9-ol (30.0 g, 88 mmol) in THF (200 mL), and the mixture was warmed to 40 °C. HCl (4 M in dioxane) (4.4 mL, 17.7 mmol) was added in four portions every 20 min and stirred for an additional 30 min. The reaction was monitored by TLC (3:1 hexanes:EtOAc, starting material R_f = 0.5, product R_f = 0.7). The solution was cooled to RT and slowly added via addition funnel to a prestirred mixture of silver cyanate (39.8 g, 265 mmol) and iodine (23.6 g, 93 mmol) in 400 mL of THF that was cooled to −30 °C (dry ice acetonitrile bath) and had been stirring for 30 min in a 2 L three-neck flask equipped with an overhead stirrer. The mixture was stirred for another 30 min at −30 °C after the addition was complete (addition over 10 min). Ammonia (2 M solution in 2-propanol) (221 mL, 442 mmol) was then added, and the dark mixture was stirred at room temperature for 20 h. The mixture was filtered and concentrated in vacuo to ca. 100 mL. The solution was diluted with EtOAc and washed with aqueous sodium thiosulfate, water, and brine, then dried over sodium sulfate and concentrated. The semisolid was diluted with ether (ca. 100 mL) and toluene (100 mL). Precipitated solid was collected by filtration to afford 20.0 g of crude product. The mother liquors were concentrated and purified by silica gel chromoatography using 2−6% MeOH in DCM with 1% NH_4OH to a material (4.0 g). Total yield of racemic **6e**: 24.0 g (53%). Racemic material was separated by SFC on 25 mm × 200 mm Chiralpak AD-H column using 25% MeOH (+0.1% diethylamine)/CO_2 to afford 8.9 g (19% yield) of first eluting peak ((*R*)-enantiomer) and 9.0 g (20% yield) of second eluting peak ((*S*)-enantiomer, desired). ^{1}H NMR (400 MHz, DMSO-d_6) δ ppm 7.51 (dd, J = 8.7, 2.5 Hz, 1 H), 7.40 (d, J = 2.5 Hz, 1 H), 7.19 (d, J = 8.7 Hz, 1 H), 7.00 (dd, J = 12.5, 3.0 Hz, 1 H), 6.63 (dd, J = 3.0, 1.7 Hz, 1 H), 6.60 (br s, 2 H), 4.10−4.16 (m, 2 H), 3.75 (s, 3 H). MS m/z = 379.0 $[M + H]^+$.

*(S)-2-Amino-7′-bromo-4′-fluoro-5H-spiro[oxazole-4,9′-xanthen]-2′-ol (**45**).* To a solution of (*S*)-7′-bromo-4′-fluoro-2′-methoxy-5*H*-spiro[oxazole-4,9′-xanthen]-2-amine ((*S*)-**6e**) (15.72 g, 41.5 mmol) in DCM (200 mL), boron tribromide (9.80 mL, 104 mmol) was added dropwise at room temp. The solution was stirred for 30 min, and then the flask was cooled with ice−water bath and carefully quenched by addition of satd $NaHCO_3$ solution (~50 mL). Most of DCM was removed under reduced pressure, and the precipitate was neutralized by further stirring with saturated $NaHCO_3$ solution (~200 mL) for 1 h, then filtered off, washed twice with water, and dried on air for 2 days. Yield: 14.59 g (96%). ^{1}H NMR (400 MHz, DMSO-d_6) δ ppm 9.69 (br s, 1 H), 7.48 (dd, J = 8.7, 2.4 Hz, 1 H), 7.35−7.42 (m, 1 H), 7.15 (d, J = 8.7 Hz, 1 H), 6.66 (dd, J = 12.3, 2.8 Hz, 1 H), 6.49−6.59 (m, 3 H), 4.10 (s, 2 H). MS m/z = 365.0 $[M + H]^+$.

*(S)-2-Amino-4′-fluoro-7′-(2-fluoropyridin-3-yl)-5H-spiro[oxazole-4,9′-xanthen]-2′-ol (**46**).* A round-bottom flask was charged with (*S*)-2-amino-7′-bromo-4′-fluoro-5*H*-spiro[oxazole-4,9′-xanthen]-2′-ol (**45**) (10.00 g, 27.4 mmol), 2-fluoropyridin-3-ylboronic acid (6.95 g, 49.3 mmol), and sodium carbonate (8.71 g, 82 mmol). DMF (80 mL) was added, and the mixture was stirred for 1 min. Tetrakis-(triphenylphosphine) palladium(0) (1.582 g, 1.369 mmol) and water (30 mL) were added, the mixture was capped with argon, the flask was equipped with reflux condenser with argon inlet, and the mixture was stirred at 85 °C for 16 h. The mixture was cooled to room temperature, and yellow precipitate was filtered off and washed with DMF. The filtrate was poured into a stirred semisaturated ammonium chloride solution (300 mL), and the mixture was stirred for 2 h at room temperature. The precipitated solid was filtered off and was washed with water and dried overnight to afford (*S*)-2-amino-4′-fluoro-7′-(2-fluoropyridin-3-yl)-5*H*-spiro[oxazole-4,9′-xanthen]-2′-ol (**46**) (9.09 g, 23.84 mmol, 87% yield) as a tan solid which was used without further purification. Purity by HPLC 90%. ^{1}H NMR (400 MHz, DMSO-d_6) δ ppm 9.71 (br s, 1 H), 8.24 (dt, J = 4.8, 1.6 Hz, 1 H), 8.10 (ddd, J = 10.3, 7.3, 2.0 Hz, 1 H), 7.54−7.62 (m, 2 H), 7.48 (ddd, J = 7.3, 5.0, 2.0 Hz, 1 H), 7.28−7.36 (m, 1 H), 6.69 (dd, J = 12.3, 2.8 Hz, 1 H), 6.60 (dd, J = 2.8, 1.5 Hz, 1 H), 6.52 (br s, 2 H), 4.10−4.21 (m, 2 H). MS m/z = 382.0 $[M + H]^+$.

*(S)-2-Amino-5′-fluoro-2′-(2-fluoropyridin-3-yl)-5H-spiro[oxazole-4,9′-xanthene]-7′-yl trifluoromethanesulfonate (**47**).* To a solution of (*S*)-2-amino-4′-fluoro-7′-(2-fluoropyridin-3-yl)-5*H*-spiro[oxazole-4,9′-xanthen]-2′-ol (**46**) (2.62 g, 6.87 mmol) in DCM (35 mL) was added triethylamine (1.39 g, 13.74 mmol), and the mixture was cooled to 0 °C. *N*-(5-Chloro-2-pyridyl)bis(trifluoromethanesulfonamide) (2.97 g, 7.56

dx.doi.org/10.1021/jm501266w | J. Med. Chem. XXXX, XXX, XXX−XXX

mmol) was added, and the mixture was stirred for 24 h at room temperature. The mixture was washed with 1N NaOH solution twice, filtered through Celite, and concentrated. The residue was purified by silica gel chromatography (0−50% DCM/MeOH/NH_4OH 90:10:1 in DCM) to afford (*S*)-2-amino-5′-fluoro-2′-(2-fluoropyridin-3-yl)-5*H*-spiro[oxazole-4,9′-xanthene]-7′-yl trifluoromethanesulfonate (**47**) (2.98 g, 5.80 mmol, 84% yield) as yellow foam. ^{1}H NMR (400 MHz, $CDCl_3$) δ ppm 8.20 (d, J = 4.5 Hz, 1 H), 7.75−7.86 (m, 1 H), 7.59 (s, 1 H), 7.54 (d, J = 8.6 Hz, 1 H), 7.28−7.31 (m, 1 H), 6.96−7.19 (m, 4 H), 6.73 (d, J = 8.0 Hz, 1 H), 6.28 (br s, 2 H), 4.42 (d, J = 8.8 Hz, 1 H), 4.36 (d, J = 8.8 Hz, 1 H). MS m/z = 513.8 $[M + H]^+$.

*Typical Procedure for Preparation of Compounds with O-Linked P2′ Groups: (S)-4′-Fluoro-2′-(2-fluoro-2-methylpropoxy)-7′-(2-fluoropyridin-3-yl)-5H-spiro[oxazole-4,9′-xanthen]-2-amine (**38**).* To a round-bottom flask were added 2-fluoro-2-methylpropyl trifluoromethanesulfonate (176 mg, 0.787 mmol), (*S*)-2-amino-4′-fluoro-7′-(2-fluoropyridin-3-yl)-5*H*-spiro[oxazole-4,9′-xanthen]-2′-ol (**46**) (250 mg, 0.656 mmol), cesium carbonate (427 mg, 1.311 mmol), and sodium iodide (44.2 mg, 0.295 mmol) in DMF (2 mL). The mixture was purged with nitrogen and stirred at room temperature for 18 h. The mixture was then diluted with water and extracted with EtOAc. The organic layer was washed with brine, filtered through Celite, and concentrated. The crude material was purified by silica gel chromatography (0−25−50% DCM/MeOH/NH_4OH (90:10:1) in 40% EtOAc in hexanes) to provide (*S*)-4′-fluoro-2′-(2-fluoro-2-methylpropoxy)-7′-(2-fluoropyridin-3-yl)-5*H*-spiro[oxazole-4,9′-xanthen]-2-amine (**38**) (179 mg, 0.393 mmol, 60% yield) as a white solid. ^{1}H NMR (400 MHz, DMSO-d_6) δ ppm 8.23−8.26 (m, 1 H), 8.07−8.13 (m, 1 H), 7.54−7.65 (m, 4 H), 7.49 (ddd, J = 7.3, 5.0, 1.9 Hz, 1 H), 7.34 (d, J = 8.4 Hz, 1 H), 7.08 (dd, J = 12.5, 2.9 Hz, 1 H), 6.70 (dd, J = 2.8, 1.5 Hz, 1 H), 6.53 (s, 2 H), 4.16−4.24 (m, 2 H), 3.93−4.10 (m, 2 H), 1.39−1.47 (m, 6 H). MS m/z = 456.0 $[M + H]^+$.

*(S)-4′-Fluoro-7′-(2-fluoropyridin-3-yl)-2′-((3-methyloxetan-3-yl)methoxy)-5H-spiro[oxazole-4,9′-xanthen]-2-amine (**37**).* Prepared from (*S*)-2-amino-4′-fluoro-7′-(2-fluoropyridin-3-yl)-5*H*-spiro[oxazole-4,9′-xanthen]-2′-ol (**46**) (58 mg, 0.152 mmol)) as described for **38** using 3-(bromomethyl)-3-methyloxetane (16 μL, 0.167 mmol) and cesium carbonate (99 mg, 0.304 mmol) in 1 mL of DMF. Yield: 25 mg (35%). ^{1}H NMR (400 MHz, DMSO-d_6) δ ppm 8.25 (d, J = 4.7 Hz, 1 H), 8.06−8.15 (m, 1 H), 7.55−7.63 (m, 2 H), 7.49 (t, J = 5.4 Hz, 1 H), 7.35 (d, J = 8.4 Hz, 1 H), 7.09 (dd, J = 12.6, 2.6 Hz, 1 H), 6.72 (br s, 1 H), 6.53 (br s, 1 H), 4.50 (d, J = 5.8 Hz, 2 H), 4.31 (d, J = 5.9 Hz, 2 H), 4.22 (d, J = 5.7 Hz, 2 H), 4.06 (q, J = 9.2 Hz, 2 H), 1.37 (s, 3 H). MS m/z = 466.0 $[M + H]^+$.

*General Procedure for Suzuki Coupling of Intermediate **63**: (S)-2′-(3,6-Dihydro-2H-pyran-4-yl)-4′-fluoro-7′-(2-fluoropyridin-3-yl)-5H-spiro[oxazole-4,9′-xanthen]-2-amine (**40**).* A 50 mL round-bottom flask was charged with (*S*)-2-amino-5′-fluoro-2′-(2-fluoropyridin-3-yl)-5*H*-spiro[oxazole-4,9′-xanthene]-7′-yl trifluoromethanesulfonate (**47**) (1.966 g, 3.83 mmol), 2-(3,6-dihydro-2*H*-pyran-4-yl)-4,4,5,5-tetramethyl-1,3,2-dioxaborolane (1.126 g, 5.36 mmol), tetrakis(triphenylphosphine)palladium(0) (0.443 g, 0.383 mmol), sodium carbonate (1.624 g, 15.32 mmol), DMF (14 mL), and water (5 mL). The mixture was heated at 85 °C overnight under positive pressure of argon. The reaction mixture was cooled to rt and filtered, and the precipitate was washed with water. The filtrate was diluted with water (∼20 mL), and precipitated material was filtered and washed with water. The solids were combined, redissolved in DCM, dried, and concentrated. The crude material was purified by silica gel chromatography (10−60% DCM/MeOH/NH_4OH 90:10:1 in DCM) to afford (*S*)-2′-(3,6-dihydro-2*H*-pyran-4-yl)-4′-fluoro-7′-(2-fluoropyridin-3-yl)-5*H*-spiro[oxazole-4,9′-xanthen]-2-amine (**40**) (1.05 g, 2.347 mmol, 61% yield). ^{1}H NMR (400 MHz, DMSO-d_6) δ ppm 8.25 (dt, J = 4.8, 1.5 Hz, 1 H), 8.12 (ddd, J = 10.3, 7.5, 2.0 Hz, 1 H), 7.57−7.65 (m, 2 H), 7.50 (ddd, J = 7.3, 5.0, 2.0 Hz, 1 H), 7.45 (dd, J = 12.4, 2.2 Hz, 1 H), 7.38 (d, J = 8.5 Hz, 1 H), 7.21 (s, 1 H), 6.52 (s, 2 H), 6.22−6.32 (m, 1 H), 4.25 (s, 4 H), 3.77−3.87 (m, 2 H), 2.36−2.47 (m, 2 H). MS m/z = 448.0 $[M + H]^+$.

*(S)-2′-(5,6-Dihydro-2H-pyran-3-yl)-4′-fluoro-7′-(2-fluoropyridin-3-yl)-5H-spiro[oxazole-4,9′-xanthen]-2-amine (**39**).* Prepared from (*S*)-2-amino-5′-fluoro-2′-(2-fluoropyridin-3-yl)-5*H*-spiro[oxazole-4,9′-xanthene]-7′-yl trifluoromethanesulfonate (**47**) (800 mg, 1.558 mmol), as described for **49** using 2-(5,6-dihydro-2*H*-pyran-3-yl)-4,4,5,5-tetramethyl-1,3,2-dioxaborolane (655 mg, 3.12 mmol) and tetrakis(triphenylphosphine)palladium(0) (90 mg, 0.078 mmol) in DMF (5 mL) and 5 M sodium carbonate solution (1.56 mL, 7.79 mmol). Yield: 185 mg (27%). ^{1}H NMR (400 MHz, DMSO-d_6) δ ppm 8.25 (dd, J = 4.8, 1.4 Hz, 1 H), 8.08−8.15 (m, 1 H), 7.57−7.64 (m, 2 H), 7.49 (ddd, J = 7.3, 5.0, 1.8 Hz, 1 H), 7.34−7.40 (m, 2 H), 7.11 (s, 1 H), 6.51 (br s, 2 H), 6.26−6.31 (m, 1 H), 4.31−4.49 (m, 2 H), 4.23 (s, 2 H), 3.74 (t, J = 5.5 Hz, 2 H), 2.20−2.32 (m, 2 H). m/z = 448.0 $[M + H]^+$.

*General Procedure for Pd-Catalyzed Amination of Intermediate **47**: (S)-4′-Fluoro-7′-(2-fluoropyridin-3-yl)-2′-morpholino-5H-spiro[oxazole-4,9′-xanthen]-2-amine (**41**).* A resealable vial was charged with (*S*)-2-amino-5′-fluoro-2′-(2-fluoropyridin-3-yl)-5*H*-spiro[oxazole-4,9′-xanthene]-7′-yl trifluoromethanesulfonate (**47**) (200 mg, 0.390 mmol), Pd_2dba_3 (18 mg, 0.019 mmol), biphenyl-2-yldi-*tert*-butylphosphine (14 mg, 0.047 mmol), and morpholine (85 mg, 0.974 mmol). LiHMDS (1 M in THF) (1.17 mL, 1.17 mmol) was added, and the mixture was heated in microwave reactor for 1 h at 110 °C. The reaction mixture was diluted with water and extracted with ethyl acetate. The organic layer was washed with water and brine and concentrated in vacuo. The residue was purified via preparative HPLC (gradient elution 20−90% MeCN/H_2O, 0.1% TFA) followed by silica gel column chromatography using 10−90% 90/10/1 DCM/MeOH/NH_4OH in DCM to afford (*S*)-4′-fluoro-7′-(2-fluoropyridin-3-yl)-2′-morpholino-5*H*-spiro[oxazole-4,9′-xanthen]-2-amine (**41**) (20 mg, 0.044 mmol, 11% yield) as a white solid. ^{1}H NMR (400 MHz, DMSO-d_6) δ ppm 8.20−8.27 (m, 1 H), 8.05−8.13 (m, 1 H), 7.52−7.60 (m, 2 H), 7.48 (ddd, J = 7.3, 5.0, 1.9 Hz, 1 H), 7.32 (d, J = 8.5 Hz, 1 H), 6.99 (dd, J = 13.9, 2.8 Hz, 1 H), 6.64 (d, J = 1.7 Hz, 1 H), 6.48 (s, 2 H), 4.18 (s, 2 H), 3.74 (t, J = 4.6 Hz, 4 H), 3.01−3.12 (m, 4 H). MS m/z = 451.0 $[M + H]^+$.

*(S)-4′-Fluoro-7′-(2-fluoropyridin-3-yl)-2′-((S)-3-fluoropyrrolidin-1-yl)-5H-spiro[oxazole-4,9′-xanthen]-2-amine (**42**).* Prepared as described for **41** using (*S*)-2-amino-5′-fluoro-2′-(2-fluoropyridin-3-yl)-5*H*-spiro[oxazole-4,9′-xanthene]-7′-yl trifluoromethanesulfonate (**47**) (300 mg, 0.584 mmol), (*S*)-3-fluoropyrrolidine hydrochloride (367 mg, 2.92 mmol), $Pd_2(dba)_3$ (27 mg, 0.029 mmol), biphenyl-2-yldi-*tert*-butylphosphine (21 mg, 0.070 mmol), and LHMDS (1 M in THF) (4.97 mL, 4.97 mmol). Yield: 82 mg (31%). ^{1}H NMR (400 MHz, DMSO-d_6) δ ppm 8.20−8.27 (m, 1 H), 8.10 (t, J = 8.2 Hz, 1 H), 7.58 (br s, 2 H), 7.48 (ddd, J = 7.3, 5.0, 1.9 Hz, 1 H), 7.27−7.36 (m, 1 H), 6.37−6.70 (m, 3 H), 6.29 (br s, 1 H), 5 (dm, J = 54.4 Hz 1 H), 4.21 (m, 2 H), 3.31−3.60 (m, 4 H), 2.08−2.30 (m, 2 H). MS m/z = 453.2 $[M + H]^+$.

*(S)-4′-Fluoro-7′-(2-fluoropyridin-3-yl)-2′-(1-methyl-1H-pyrazol-4-yl)-5H-spiro[oxazole-4,9′-xanthen]-2-amine (**43**).* Prepared as described for **40** from (*S*)-2-amino-5′-fluoro-2′-(2-fluoropyridin-3-yl)-5*H*-spiro[oxazole-4,9′-xanthene]-7′-yl trifluoromethanesulfonate (**47**) (100 mg, 0.195 mmol), tetrakis(triphenylphosphine)palladium(0) (23 mg, 0.019 mmol), 1-methyl-4-(4,4,5,5-tetramethyl-1,3,2-dioxaborolan-2-yl)-1*H*-pyrazole (81 mg, 0.380 mmol), and 5 M sodium carbonate solution (0.2 mL, 0.974 mmol) in DMF (2 mL); isolated by preparative HPLC (gradient elution 20−90% MeCN/H_2O, 0.1% TFA) as TFA salt. Yield 65 mg (61%). ^{1}H NMR (400 MHz, DMSO-d_6) δ ppm 11.12 (br s, 1 H), 9.32−9.69 (m, 2 H), 8.15−8.33 (m, 3 H), 7.98 (s, 1 H), 7.61−7.85 (m, 3 H), 7.44−7.57 (m, 2 H), 5.17 (m, 2 H), 3.88 (s, 3 H). MS m/z = 446.0 $[M + H]^+$.

*(S)-4′-Fluoro-7′-(2-fluoropyridin-3-yl)-2′-(pyridin-2-yl)-5H-spiro[oxazole-4,9′-xanthen]-2-amine (**44**).* A resealable vial was charged with (*S*)-2-amino-5′-fluoro-2′-(2-fluoropyridin-3-yl)-5*H*-spiro[oxazole-4,9′-xanthene]-7′-yl trifluoromethanesulfonate (**47**) (100 mg, 0.195 mmol), tetrakis(triphenylphosphine)palladium(0) (23 mg, 0.019 mmol), and pyridin-2-ylzinc(II) bromide (0.5 M in THF) (1.95 mL, 0.974 mmol). The vial was sealed and heated at 70 °C for 5 h. The reaction was quenched by addition of 1 mL of saturated aq NH_4Cl and extracted with ethyl acetate. The organic layer was concentrated, and the residue was purified by silica gel chromatography (10−80% DCM/MeOH/NH_4OH 90:10:1 in DCM). Yield: 62 mg (72%). ^{1}H NMR (400 MHz, DMSO-d_6) δ ppm 8.67−8.71 (m, 1 H), 8.25 (dt, J = 4.8, 1.5 Hz, 1 H), 8.13 (ddd, J = 10.3, 7.5, 1.9 Hz, 1 H), 8.00−8.05 (m, 2 H), 7.95−7.99

dx.doi.org/10.1021/jm501266w | J. Med. Chem. XXXX, XXX, XXX−XXX

(m, 1 H), 7.88−7.94 (m, 1 H), 7.60−7.66 (m, 2 H), 7.50 (ddd, J = 7.3, 5.0, 2.0 Hz, 1 H), 7.35−7.43 (m, 2 H), 6.55 (br s, 2 H), 4.30 (s, 2 H). MS m/z = 443.0 $[M + H]^+$.

BACE1 Enzymatic Assay. BACE1 enzymatic activity was determined by the enhancement of fluorescence intensity upon enzymatic cleavage of the fluorescence resonance energy transfer substrate according to the previously published procedure.[8d]

Cell-Based Assay. BACE 1 cellular activity was determined in human embryonic kidney cells (HEK293) stably expressing APP_{SW}. After incubation overnight with the test compounds, the conditioned media was collected and the Aβ40 levels were determined using a sandwich ELISA as described previously.[8d]

Permeability assay was performed in the wild-type cell line LLC-PK1 (porcine renal epithelial cells, WT-LLC-PK1) transfected with human *MDR*1 gene (hMDR1-LLC-PK1) and rat *mdr1a* gene (rMdr1a-LLC-PK1) as described previously.[8d]

Microsomal Stability Assay. Compounds (1 μM) were incubated with liver microsomes from human and rat for 30 min at 37 °C, and the samples were analyzed according to published procedure.[13]

hERG Binding Assay. A stable HEK293 cell line expressing the hERG channel was established in-house. Compounds were tested in the [^{3}H]-dofetilide binding assay with cell membranes prepared from this cell line using method of Finlayson with some modifications.[41] Briefly, filtration assays were carried out in 194 μL of binding buffer (10 mM HEPES, pH 7.4, 60 mM KCl, 71.5 mM NaCl, 1 mM $CaCl_2$, 2 mM $MgCl_2$) with 10 μg/well membrane (based on membrane protein) and [^{3}H]-dofetilide (8 nM) and 6 μL of compound dissolved in 100% DMSO. Nonspecific binding was determined by using 10 μM cold dofetilide (~1000-fold molar excess over hot ligand). The entire assay was conducted in 96-well Whatman Unifilter plates at room temperature for 90 min. The binding assay was terminated by washing the plates four times on a Millipore Vacuum filtration manifold with 100 μL/well of ice cold wash buffer (10 mM HEPES, pH 7.4, 131.5 mM NaCl, 1 mM $CaCl_2$, 2 mM $MgCl_2$). The bound radioisotope was quantified using a Packard TopCount NTS liquid scintillation counter with scintillation fluid.

Rat Pharmacodynamic Assay. Male Sprague−Dawley rats (175−200 g) were administered compound by oral gavage at the appropriate dose. Samples of plasma, CSF, and brain were analyzed according to reported procedures.[13]

Dog Cardiovascular Safety Studies. *Animal Preparation.* Male beagle dogs (10−12 kg) were anesthetized with 2 mg/kg morphine, dosed subcutaneously, followed by a 110 mg/kg intravenous bolus of α-chloralose. After induction, animals were intubated and ventilated at an appropriate rate and volume with ambient air. Maintenance on surgical plane was achieved with a constant infusion of 45 mg/kg/h of α-chloralose. Animals were kept on a thermal blanket and heat lamp to maintain normal body temperature and monitored throughout the study by veterinary staff. The study was conducted with approval of the Institutional Animal Care and Use Committee.

Cardiovascular Monitoring. Arterial pressure and heart rate were measured directly from a femoral artery catheter and catheters were placed in both femoral veins for infusion of drug and blood sampling, using standard surgical techniques. ECG signals (l II and V) were captured simultaneously from subcutaneous limb and precordial needle electrodes, respectively. After surgery, the animals were allowed to stabilize for a minimum of 45 min prior to collecting pretreatment (baseline) data. After baseline values were collected, the test article was administered in a rising-dose paradigm in which vehicle and escalating doses were infused intravenously. Each dose (vehicle or test article) was given over 30 min. Animals were euthanized at the conclusion of the study.

Data Acquisition and Analysis. A computerized data acquisition system (CARecorder; DISS, Inc.) was used to collect all raw input signals. Arterial pressure, heart rate, and cardiac intervals were recorded continuously throughout the study and averaged at 30 s intervals. All raw data were converted with EMKA ecg-auto (version 2.5.1.30; Paris, France) into *.d01 files for analysis purposes. In the tables, values were compared to end of vehicle infusion. Data were analyzed using ecg-auto v2.5.1.30 (EMKA Technologies).

Isolated Rabbit Heart Using Langendorff Perfusion. All rabbit experiments were conducted in compliance with the Amgen Institutional Animal Care and Use Committee and USDA regulations.

Isolated rabbit heart experiments were performed using procedure described by Qu et al.[42] using 0.3, 1, 3, and 10 μM solutions of compound **2** or 0.1, 0.3, 1, 3, and 10 μM solutions of compound **40** were tested under constant flow condition, with each concentration applied for 20 min.

Cocrystallization of BACE1 Complexes. The extracellular domain of BACE1 was expressed, purified, and crystallized according to published procedures.[43] Inhibitor complexes were obtained by soaking apo BACE1 crystals in mother liquor solutions supplemented with 0.5 mM compound **40** or 1 mM compound **2** for a period of ~3 h. Crystals were transferred briefly into a cryo solution consisting of 25% (w/v) PEG 5000 MME, 0.1 M sodium citrate (pH 6.6), 0.2 M ammonium iodide, and 20% (v/v) glycerol prior to being flash frozen in liquid nitrogen. Diffraction data were collected either on an FR-E rotating anode X-ray source equipped with an RAXIS IV++ detector (compound **2**) or at beamline 5.0.1 of the Advanced Light Source using an ADSC Q315R CCD detector and λ = 0.97741 Å (compound **40**). Images were processed using the HKL suite of programs.[44] The structures were refined using REFMAC,[45] and model building was performed with COOT.[46] Data collection and refinement statistics appear in the Supporting Information.

■ ASSOCIATED CONTENT

Ⓢ Supporting Information

Synthetic procedures and analytical data for test compounds and synthetic procedures for intermediates, ^{1}H and ^{13}C NMR spectra of compound **40**, BACE1 enzyme data and calculated LogP and PSA for compounds **37**−**44**, determination of IC_{50}, and data collection and refinement statistics for cocrystals of **2** and **40** with BACE1. This material is available free of charge via the Internet at http://pubs.acs.org.

Accession Codes

New protein/ligand coordinates for **2** and **40** with BACE1 have been deposited in the PDB with IDs 4RCE and 4RCF.

■ AUTHOR INFORMATION

Corresponding Author

*Phone: 1-617-444-5353. E-mail: oepstein@amgen.com. Address: Department of Medicinal Chemistry, Amgen Inc., 360 Binney Street, Cambridge, Massachusetts 02142, United States.

Present Addresses

[#]For M. C. B.: Genentech, Inc., 1 DNA Way, South San Francisco, California 94080, United States.

[▽]For V. F. P.: Sanofi-Aventis, 153 Second Avenue, Waltham, Massachusetts 02451, United States.

Notes

The authors declare no competing financial interest.

■ ACKNOWLEDGMENTS

We thank Matthew Potter, Grace Bi, and Larry Miller for chiral separation, Jie Yan and Michele Kubryk for help with resynthesis of the lead compounds for safety studies, and Alexander M. Long for purification of BACE1 protein. We also thank Kui Chen, Steven Louie, Joel Esmay, and Yi Luo for in vitro screening of the test compounds and Yusheng Qu, Mei Fang, BaoXi Gao, and Shanti Amagasu for ex vivo safety studies.

■ ABBREVIATIONS USED

hERG, human ether-a-go-go-related gene; BACE1, β-site APP cleaving enzyme; AD, Alzheimer's disease; Pgp, P-glycoprotein; Aβ, β-amyloid; APP, amyloid-β precursor protein; CNS, central

nervous system; PD, pharmacodynamic; IRH, isolated rabbit heart; QTc, corrected QT interval; K_i, absolute inhibition constant; DCM, dichloromethane; TLC, thin layer chromatography

REFERENCES

(1) *2014 Alzheimer's Disease Facts and Figures*; Alzheimer's Association: Chicago, 2014; http://www.alz.org/downloads/facts_figures_2014.pdf.

(2) Citron, M. Alzheimer's disease: strategies for disease modification. *Nature Rev. Drug Discovery* **2010**, *9*, 387−398.

(3) (a) Hardy, J.; Selkoe, D. J. The amyloid hypothesis of Alzheimer's disease: progress and problems on the road to therapeutics. *Science* **2002**, *297*, 353−356. (b) Querfurth, H. W.; LaFerla, F. M. Mechanisms of Disease: Alzheimer's disease. *N. Engl. J. Med.* **2010**, *362*, 329−344.

(4) Haass, C.; Lemere, C. A.; Capell, A.; Citron, M.; Seubert, P.; Schenk, D.; Lannfelt, L.; Selkoe, D. J. The Swedish mutation causes early-onset Alzheimer's disease by β-secretase cleavage within the secretory pathway. *Nature Med.* **1995**, *1*, 1291−1296.

(5) Jonsson, T.; Atwal, J. K.; Steinberg, S.; Snaedal, J.; Jonsson, P. V.; Bjornsson, S.; Stefansson, H.; Sulem, P.; Gudbjartsson, D.; Maloney, J.; Hoyte, K.; Gustafson, A.; Liu, Y.; Lu, Y.; Bhangale, T.; Graham, R. R.; Huttenlocher, J.; Bjornsdottir, G.; Andreassen, O. A.; Jönsson, E. G.; Palotie, A.; Behrens, T. W.; Magnusson, O. T.; Kong, A.; Thorsteinsdottir, U.; Watts, R. J.; Stefansson, K. A mutation in APP protects against Alzheimer's disease and age-related cognitive decline. *Nature* **2012**, *488*, 96−99.

(6) (a) Vassar, R.; Bennett, B. D.; Babu-Khan, S.; Kahn, S.; Mendiaz, E. A.; Denis, P.; Teplow, D. B.; Ross, S.; Amarante, P.; Loeloff, R.; Luo, Y.; Fisher, S.; Fuller, J.; Edenson, S.; Lile, J.; Jarosinski, M. A.; Biere, A. L.; Curran, E.; Burgess, T.; Louis, J. C.; Collins, F.; Treanor, J.; Rogers, G.; Citron, M. Beta-Secretase Cleavage of Alzheimer's Amyloid Precursor Protein by the Transmembrane Aspartic Protease BACE. *Science* **1999**, *286*, 735−741. (b) Hussain, I.; Powell, D.; Howlett, D. R.; Tew, D. G.; Meek, T. D.; Chapman, C.; Gloger, I. S.; Murphy, K. E.; Southan, C. D.; Ryan, D. M.; Smith, T. S.; Simmons, D. L.; Walsh, F. S.; Dingwall, C.; Christie, G. Identification of a Novel Aspartic Protease (Asp 2) as beta-Secretase. *Mol. Cell Neurosci.* **1999**, *14*, 419−427. (c) Yan, R.; Bienkowski, M. J.; Shuck, M. E.; Miao, H.; Tory, M. C.; Pauley, A. M.; Brashier, J. R.; Stratman, N. C.; Mathews, W. R.; Buhl, A. E.; Carter, D. B.; Tomasselli, A. G.; Parodi, L. A.; Heinrikson, R. L.; Gurney, M. E. Membraned-Anchored Aspartyl Protease with Alzheimer's Disease b-Secretase Activity. *Nature* **1999**, *402*, 533−537. (d) Sinha, S.; Anderson, J. P.; Barbour, R.; Basi, G. S.; Caccavello, R.; Davis, D.; Doan, M.; Dovey, H. F.; Frigon, N.; Hong, J.; Jacobson-Croak, K.; Jewett, N.; Keim, P.; Knops, J.; Lieberburg, I.; Power, M.; Tan, H.; Tatsuno, G.; Tung, J.; Schenk, D.; Seubert, P.; Suomensaari, S. M.; Wang, S.; Walker, D.; Zhao, J.; McConlogue, L.; John, V. *Nature* **1999**, *402*, 537−540.

(7) For review, see: Beck, J. P.; Mergott, D. J. Peptidic, peptidomimetic, and HTS-derived BACE inhibitors. In *BACE: Lead Target for Orchestrated Therapy of Alzheimer'S Disease*; John, V., Ed.; John Wiley & Sons, Inc.: New York, 2010; pp 59−105.

(8) For recent reports, see: (a) Rueeger, H.; Lueoend, R.; Machauer, R.; Veenstra, S. J.; Jacobson, L. H.; Staufenbiel, M.; Desrayaud, S.; Rondeau, J.-M.; Mobitz, H.; Neumann, U. Discovery of cyclic sulfoxide hydroxyethylamines as potent and selective β-site APP-cleaving enzyme 1 (BACE1) inhibitors: structure based design and in vivo reduction of amyloid β-peptides. *Bioorg. Med. Chem. Lett.* **2013**, *23*, 5300−5306. (b) Ng, R. A.; Sun, M.; Bowers, S.; Hom, R. K.; Probst, G. D.; John, V.; Fang, L. Y.; Maillard, M.; Gailunas, A.; Brogley, L.; Neitz, R. J.; Tung, J. S.; Pleiss, M. A.; Konradi, A. W.; Sham, H. L.; Dappen, M. S.; Adler, M.; Yao, N.; Zmolek, W.; Nakamura, D.; Quinn, K. P.; Sauer, J.-M.; Bova, M. P.; Ruslim, L.; Artis, D. R.; Yednock, T. A. Design and synthesis of hydroxyethylamine (HEA) BACE-1 inhibitors: prime side chromane-containing inhibitors. *Bioorg. Med. Chem. Lett.* **2013**, *23*, 4674−4679. (c) Weiss, M. M.; Williamson, T.; Babu-Khan, S.; Bartberger, M. D.; Brown, J.; Chen, K.; Cheng, Y.; Citron, M.; Croghan, M. D.; Dineen, T. A.; Esmay, J.; Graceffa, R. F.; Harried, S. S.; Hickman, D.; Hitchcock, S. A.; Horne, D. B.; Huang, H.; Imbeah-Ampiah, R.; Judd, T.; Kaller, M. R.; Kreiman, C. R.; La, D. S.; Li, V.; Lopez, P.; Louie, S.; Monenschein, H.; Nguyen, T. T.; Pennington, L. D.; Rattan, C.; San Miguel, T.; Sickmier, E. A.; Wahl, R. C.; Wen, P. H.; Wood, S.; Xue, Q.; Yang, B. H.; Patel, V. F.; Zhong, W. Design and Preparation of a Potent Series of Hydroxyethylamine Containing β-Secretase Inhibitors That Demonstrate Robust Reduction of Central β-Amyloid. *J. Med. Chem.* **2012**, *55*, 9009−9024. (d) Dineen, T. A.; Weiss, M. M.; Williamson, T.; Acton, P.; Babu-Khan, S.; Bartberger, M. D.; Brown, J.; Chen, K.; Cheng, Y.; Citron, M.; Croghan, M. D.; Dunn, R. T.; Esmay, J.; Graceffa, R. F.; Harried, S. S.; Hickman, D.; Hitchcock, S. A.; Horne, D. B.; Huang, H.; Imbeah-Ampiah, R.; Judd, T.; Kaller, M. R.; Kreiman, C. R.; La, D. S.; Li, V.; Lopez, P.; Louie, S.; Monenschein, H.; Nguyen, T. T.; Pennington, L. D.; San Miguel, T.; Sickmier, E. A.; Vargas, H. M.; Wahl, R. C.; Wen, P. H.; Whittington, D. A.; Wood, S.; Xue, Q.; Yang, B. H.; Patel, V. F.; Zhong, W. Design and Synthesis of Potent, Orally Efficacious Hydroxyethylamine Derived β-Site Amyloid Precursor Protein Cleaving Enzyme (BACE1) Inhibitors. *J. Med. Chem.* **2012**, *55*, 9025−9044. (e) Rueeger, H.; Rondeau, J.-M.; McCarthy, C.; Möbitz, H.; Tintelnot-Blomley, M.; Neumann, U.; Desrayaud, S. Structure based design, synthesis and SAR of cyclic hydroxyethylamine (HEA) BACE-1 inhibitors. *Bioorg. Med. Chem. Lett.* **2011**, *21*, 1942−1947. (f) Marcin, L. R.; Higgins, M. A.; Zusi, F. C.; Zhang, Y.; Dee, M. F.; Parker, M. F.; Muckelbauer, J. K.; Camac, D. M.; Morin, P. E.; Ramamurthy, V.; Tebben, A. J.; Lentz, K. A.; Grace, J. E.; Marcinkeviciene, J. A.; Kopcho, L. M.; Burton, C. R.; Barten, D. M.; Toyn, J. H.; Meredith, J. E.; Albright, C. F.; Bronson, J. J.; Macor, J. E.; Thompson, L. A. Synthesis and SAR of indole- and 7-azaindole-1,3-dicarboxamide hydroxyethylamine inhibitors of BACE-1. *Bioorg. Med. Chem. Lett.* **2011**, *21*, 537−541.

(9) For reviews see: (a) Zhu, Z. Iminoheterocycle as a druggable motif: BACE1 inhibitors and beyond. *Trends Pharmacol. Sci.* **2012**, *33*, 233−240. (b) Oehlrich, D.; Prokopcova, H.; Gijsen, H. J. M. The evolution of amidine-based brain penetrant BACE1 inhibitors. *Bioorg. Med. Chem. Lett.* **2014**, *24*, 203−2045.

(10) (a) Edwards, P. D.; Albert, J. S.; Sylvester, M.; Aharony, D.; Andisik, D.; Callaghan, O.; Campbell, J. B.; Carr, R. A.; Chessari, G.; Congreve, M.; Frederickson, M.; Folmer, R. H. A.; Geschwindner, S.; Koether, G.; Kolmodin, K.; Krumrine, J.; Mauger, R. C.; Murray, C. W.; Olsson, L. L.; Patel, S.; Spear, N.; Tian, G. Application of fragment-based lead generation to the discovery of novel, cyclic amidine β-secretase inhibitors with nanomolar potency, cellular activity, and high ligand efficiency. *J. Med. Chem.* **2007**, *50*, 5912−5925. (b) Malamas, M. S.; Erdei, J.; Gunawan, I.; Barnes, K.; Johnson, M.; Hui, Y.; Turner, J.; Hu, Y.; Wagner, E.; Fan, K.; Olland, A.; Bard, J.; Robichaud, A. J. Aminoimidazoles as potent and selective human β-secretase (BACE1) inhibitors. *J. Med. Chem.* **2009**, *52*, 6314−6323. (c) Thomas, A. A.; Hunt, K. W.; Volgraf, M.; Watts, R. J.; Liu, X.; Vigers, G.; Smith, D.; Sammond, D.; Tang, T. P.; Rhodes, S. P.; Metcalf, A. T.; Brown, K. D.; Otten, J. N.; Burkard, M.; Cox, A. A.; Do, M. K. G.; Dutcher, D.; Rana, S.; DeLisle, R. K.; Regal, K.; Wright, A. D.; Groneberg, R.; Scearce-Levie, K.; Siu, M.; Purkey, H. E.; Lyssikatos, J. P.; Gunawardana, I. W. Discovery of 7-Tetrahydropyran-2-yl Chromans: β-Site Amyloid Precursor Protein Cleaving Enzyme 1 (BACE1) Inhibitors That Reduce Amyloid β-Protein (Aβ) in the Central Nervous System. *J. Med. Chem.* **2014**, *57*, 878−902. (d) Cheng, Y.; Judd, T. C.; Bartberger, M. D.; Brown, J.; Chen, K.; Fremeau, R. T., Jr.; Hickman, D.; Hitchcock, S. A.; Jordan, B.; Li, V.; Lopez, P.; Louie, S. W.; Luo, Y.; Michelsen, K.; Nixey, T.; Powers, T. S.; Rattan, C.; Sickmier, E. A.; St. Jean, D. J., Jr.; Wahl, R. C.; Wen, P. H.; Wood, S. From fragment screening to in vivo efficacy: optimization of a series of 2-aminoquinolines as potent inhibitors of beta-site amyloid precursor protein cleaving enzyme 1 (BACE1). *J. Med. Chem.* **2011**, *54*, 5836−5857. (e) Mandal, M.; Zhu, Z.; Cumming, J. N.; Liu, X.; Strickland, C.; Mazzola, R. D.; Caldwell, J. P.; Leach, P.; Grzelak, M.; Hyde, L.; Zhang, Q.; Terracina, G.; Zhang, L.; Chen, X.; Kuvelkar, R.; Kennedy, M. E.; Favreau, L.; Cox, K.; Orth, P.; Buevich, A.; Voigt, J.; Wang, H.; Kazakevich, I.; McKittrick, B. A.; Greenlee, W.; Parker, E. M.; Stamford, A. W. Design and validation of bicyclic iminopyrimidinones as beta amyloid cleaving enzyme-1 (BACE1) inhibitors: conformational constraint to favor a bioactive conformation. *J. Med. Chem.* **2012**, *55*,

9331−9345. (f) Cumming, J. N.; Smith, E. M.; Wang, L.; Misiaszek, J.; Durkin, J.; Pan, J.; Iserloh, U.; Wu, Y.; Zhu, Z.; Strickland, C.; Voigt, J.; Chen, X.; Kennedy, M. E.; Kuvelkar, R.; Hyde, L. A.; Cox, K.; Favreau, L.; Czarniecki, M. F.; Greenlee, W. J.; McKittrick, B. A.; Parker, E. M.; Stamford, A. W. Structure based design of iminohydantoin BACE1 inhibitors: identification of an orally available, centrally active BACE1 inhibitor. *Bioorg. Med. Chem. Lett.* **2012**, *22*, 2444−2449. (g) Malamas, M. S.; Erdei, J.; Gunawan, I.; Turner, J.; Hu, Y.; Wagner, E.; Fan, K.; Chopra, R.; Olland, A.; Bard, J.; Jacobsen, S.; Magolda, R. L.; Pangalos, M.; Robichaud, A. J. Design and synthesis of 5,5′-disubstituted aminohydantoins as potent and selective human β-secretase (BACE1) inhibitors. *J. Med. Chem.* **2010**, *53*, 1146−1158.

(11) May, P. C.; Dean, R. A.; Lowe, S. L.; Martenyi, F.; Sheehan, S. M.; Boggs, L. N.; Monk, S. A.; Mathes, B. M.; Mergott, D. J.; Watson, B. M.; Stout, S. L.; Timm, D. E.; Smith Labell, E.; Gonzales, C. R.; Nakano, M.; Jhee, S. S.; Yen, M.; Ereshefsky, L.; Lindstrom, T. D.; Calligaro, D. O.; Cocke, P. J.; Hall, G. D.; Friedrich, S.; Citron, M.; Audia, J. E. Robust central reduction of amyloid-β in humans with an orally available, non-peptidic β-secretase inhibitor. *J. Neurosci.* **2011**, *31*, 16507−16516.

(12) Stone, J.; Kleijn, H. J.; Dockendorf, M.; Ma, L.; Palcza, J.; Tseng, J.; Tanen, M.; Forman, M. Consistency of Bace inhibitor-mediated brain amyloid production inhibition by MK-8931 in Alzheimer's disease patients and healthy young adults. *Alzheimer's Dementia* **2013**, *9*, P690−P691.

(13) Huang, H.; La, D. S.; Cheng, A. C.; Whittington, D. A.; Patel, V. F.; Chen, K.; Dineen, T. A.; Epstein, O.; Graceffa, R.; Hickman, D.; Kiang, Y.-H.; Louie, S.; Luo, Y.; Wahl, R. C.; Wen, P. H.; Wood, S.; Fremeau, R. T., Jr. Structure- and property-based design of amino-oxazoline xanthenes as selective, orally efficacious, and CNS penetrable BACE inhibitors for the treatment of Alzheimer's disease. *J. Med. Chem.* **2012**, *55*, 9156−9169.

(14) In this paper, substituents on the aminooxazoline xanthene core were named in accordance with the space they occupy in the catalytic domain of the BACE1 enzyme as it was determined by X-ray cocrystal structure of compound **2** with BACE1 protein. For example, the substituents binding in the S3 region of the enzyme are named P3 substituents, those binding in the S2′ region are named P2′ substituents, etc.

(15) Defined as the unbound plasma concentration corresponding to 50% brain Aβ reduction.

(16) Roden, D. M. Drug-induced prolongation of the QT interval. *N. Engl. J. Med.* **2004**, *350*, 1013−1022.

(17) The cardiac safety of **2** was tested preclinically in isolated rabbit heart (IRH) and anesthetized dog assays. In the IRH assay, hearts (n = 3) were perfused with four concentrations of **2** at increasing doses of 0.3, 1, 3, and 10 mM. Each dose was applied for 20 min with measurements collected continuously. At 10 mM, >10% prolongation of the QTc interval was observed with no effects at 3 mM. In the anesthetized dog assay, anesthetized dogs (n = 2) were treated intravenously with 30 min infusions of **2** at doses 3.5, 11.5 and 45 mg/kg. At a dose of 11.5 mg/kg ($C_{plasma,u}$ = 0.082 mM) >10% QTc widening was observed with borderline effects on QTc at 3.5 mg/kg dose ($C_{plasma,u}$ = 0.432 mM).

(18) Jamieson, C.; Moir, E. M.; Rankovic, Z.; Wishart, G. Medicinal Chemistry of hERG Optimizations: Highlights and Hang-Ups. *J. Med. Chem.* **2006**, *49*, 5029−5046.

(19) Swahn, B.-M.; Kolmodin, K.; Karlström, S.; von Berg, S.; Söderman, P.; Holenz, J.; Berg, S.; Lindström, J.; Sundström, M.; Turek, D.; Kihlström, J.; Slivo, C.; Andersson, L.; Pyring, D.; Rotticci, D.; Öhberg, L.; Kers, A.; Bogar, K.; von Kieseritzky, F.; Bergh, M.; Olsson, L.; Janson, J.; Eketjäll, S.; Georgievska, B.; Jeppsson, F.; Fälting, J. Design and synthesis of β-secretase (BACE1) inhibitors with in vivo brain reduction of β-amyloid peptides. *J. Med. Chem.* **2012**, *55*, 9346−9361.

(20) Cumming, J. G.; Tucker, H.; Oldfield, J.; Fielding, C.; Highton, A.; Faull, A.; Wild, M.; Brown, D.; Wells, S.; Shaw, J. Balancing hERG affinity and absorption in the discovery of AZD5672, an orally active CCR5 antagonist for the treatment of rheumatoid arthritis. *Bioorg. Med. Chem. Lett.* **2012**, *22*, 1655−1659.

(21) Stachel, S. J.; Coburn, C. A.; Rush, D.; Jones, K. L. G.; Zhu, H.; Rajapakse, H.; Graham, S. L.; Simon, A.; Holloway, M. K.; Allison, T. J.; Munshi, S. K.; Espeseth, A. S.; Zuck, P.; Colussi, D.; Wolfe, A.; Pietrak, B. L.; Lai, M.; Vacca, J. P. Discovery of aminoheterocycles as a novel β-secretase inhibitor class: pH dependence on binding activity part 1. *Bioorg. Med. Chem. Lett.* **2009**, *19*, 2977−2980.

(22) Swahn, B.-M.; Holenz, J.; Kihlstrom, J.; Kolmodin, K.; Lindstrom, J.; Plobeck, N.; Rotticci, D.; Sehgelmeble, F.; Sundstrom, M.; von Berg, S.; Falting, J.; Georgievska, B.; Gustavsson, S.; Neelissen, J.; Ek, M.; Olsson, L.-L.; Berg, S. Aminoimidazoles as BACE-1 inhibitors: the challenge to achieve in vivo brain efficacy. *Bioorg. Med. Chem. Lett.* **2012**, *22*, 1854−1859.

(23) Gravenfors, Y.; Viklund, J.; Blid, J.; Ginman, T.; Karlström, S.; Kihlström, J.; Kolmodin, K.; Lindström, J.; von Berg, S.; von Kieseritzky, F.; Slivo, C.; Swahn, B.-M.; Olsson, L.-L.; Johansson, P.; Eketjäll, S.; Fälting, J.; Jeppsson, F.; Strömberg, K.; Janson, J.; Rahm, F. New aminoimidazoles as β-secretase (BACE-1) inhibitors showing amyloid-β (Aβ) lowering in brain. *J. Med. Chem.* **2012**, *55*, 9297−9311.

(24) (a) Mahar Doan, K. M.; Humphreys, J. E.; Webster, L. O.; Wring, S. A.; Shampine, L. J.; Serabjit-Singh, C. J.; Adkison, K. K.; Polli, J. W. Passive Permeability and P-Glycoprotein Mediated Efflux Differentiate CNS and Non-CNS Marketed Drugs. *J. Pharmacol. Exp. Ther.* **2002**, *303*, 1029−1037. (b) Hitchcock, S. A.; Pennington, L. D. Structure−Brain Exposure Relationships. *J. Med. Chem.* **2006**, *49*, 7559−7583.

(25) Experimentally measured pK_a for compound **2** by potentiometric titration.

(26) Marcoux, J.-F.; Doye, S.; Buchwald, S. L. A General Copper-Catalyzed Synthesis of Diaryl Ethers. *J. Am. Chem. Soc.* **1997**, *119*, 10539−10540.

(27) Sousa, M. E.; Pinto, M. M. M. Synthesis of Xanthones: An Overview. *Curr. Med. Chem.* **2005**, *12*, 2447−2479.

(28) Peterson, D. J. Carbonyl olefination reaction using silyl-substituted organometallic compounds. *J. Org. Chem.* **1968**, *33*, 780−784.

(29) (a) Fernandez, J. M. G.; Mellet, C. O.; Adrian, M. A. P.; Mota, J. F. Syntheses and spectral properties of β-iodoureas and 2-amino-4,4-diphenyl-2-oxazolines. *J. Heterocycl. Chem.* **1991**, *28*, 777−780. (b) Hassner, A.; Lorber, M. E.; Heathcock, C. H. Addition of Iodine Isocyanate to Olefins. Scope and Synthetic Utility. *J. Org. Chem.* **1967**, *32*, 540−549.

(30) Miyaura, N.; Suzuki, A. Palladium-Catalyzed Cross-Coupling Reactions of Organoboron Compounds. *Chem. Rev.* **1995**, *95*, 245y−2483.

(31) Huang, H.; Liu, H.; Jiang, H.; Chen, K. Rapid and Efficient Pd-Catalyzed Sonogashira Coupling of Aryl Chlorides. *J. Org. Chem.* **2008**, *73*, 6037−6040.

(32) Guram, A. S.; King, A. O.; Allen, J. G.; Wang, X.; Schenkel, L. B.; Chan, J.; Bunel, E. E.; Faul, M. M.; Larsen, R. D.; Martinelli, M. J.; Reider, P. J. New Air-Stable Catalysts for General and Efficient Suzuki−Miyaura Cross-Coupling Reactions of Heteroaryl Chlorides. *Org. Lett.* **2006**, *9*, 1787−1789.

(33) (a) Biscoe, M. R.; Fors, B. P.; Buchwald, S. L. A New Class of Easily Activated Palladium Precatalysts for Facile C−N Cross-Coupling Reactions and the Low Temperature Oxidative Addition of Aryl Chlorides. *J. Am. Chem. Soc.* **2008**, *130*, 6686−6687. (b) Surry, D. S.; Buchwald, S. L. Dialkylbiaryl phosphines in Pd-catalyzed amination: a user's guide. *Chem. Sci.* **2011**, *2*, 27−50.

(34) For the results of introducing nitrogen atom in position 4 of the xanthene ring see: Dineen, T. A.; Chen, K.; Cheng, A. C.; Derakhchan, K.; Epstein, O.; Esmay, J.; Hickman, D.; Kreiman, C. E.; Marx, I. E.; Wahl, R. C.; Wen, P. H.; Weiss, M. M.; Whittington, D. A.; Wood, S.; Fremeau, R. T., Jr.; White, R. D.; Patel, V. F. Protein Cleaving Enzyme (BACE1): Identification of (*S*)-7-(2-fluoropyridin-3-yl)-3-((3-methyloxetan-3-yl)ethynyl)-5′*H*-spiro[chromeno[2,3-*b*]pyridine- 5,4′-oxazol]-2′-amine (AMG-8718) *J. Med. Chem.* **2014**, DOI: 10.1021/jm5012676.

(35) Mandal, M.; Zhu, Z.; Cumming, J. N.; Liu, X.; Strickland, C.; Mazzola, R. D.; Caldwell, J. P.; Leach, P.; Grzelak, M.; Hyde, L.; Zhang, Q.; Terracina, G.; Zhang, L.; Chen, X.; Kuvelkar, R.; Kennedy, M. E.; Favreau, L.; Cox, K.; Orth, P.; Buevich, A.; Voigt, J.; Wang, H.; Kazakevich, I.; McKittrick, B. A.; Greenlee, W.; Parker, E. M.; Stamford, A. W. Design and validation of bicyclic iminopyrimidinones as beta

amyloid cleaving enzyme-1 (BACE1) inhibitors: conformational constraint to favor a bioactive conformation. *J. Med. Chem.* **2012**, *55*, 9331−9345.
(36) Volgraf, M.; Chan, L.; Huestis, M. P.; Purkey, H. E.; Burkard, M.; Do, M. G.; Harris, J.; Hunt, K. W.; Liu, X.; Lyssikatos, J. P.; Rana, S.; Thomas, A. A.; Vigers, G. P. A.; Siu, M. Synthesis, characterization, and PK/PD studies of a series of spirocyclic pyranochromene BACE1 inhibitors. *Bioorg. Med. Chem. Lett.* **2014**, *24*, 2477−2480.
(37) An estimate of unbound EC_{50} for Ab lowering was calculated from a single dose, single time point (4 h) experiment assuming a standard sigmoid dose response (Hill slope of 1). This approach was initially validated by comparing EC_{50} values from a dose response experiment to the single dose, single time point estimate of unbound EC_{50}. Subsequently, estimated EC_{50}s have been shown to be a good approximation of the IC_{50} determined from a time course experiment using an indirect response PK/PD model.
(38) Potency against murine BACE1 for the series of aminooxazoline xanthenes has typically been equal to human BACE1.
(39) Bissantz, C.; Kuhn, B.; Stahl, M. A Medicinal Chemist's Guide to Molecular Interactions. *J. Med. Chem.* **2010**, *53*, 5061−5084.
(40) Felmlee, M. A.; Morris, M. E.; Mager, D. E. Mechanism-based pharmacodynamic modeling. *Methods Mol. Biol.* **2012**, *929*, 583−600 See also Supporting Information for the details..
(41) Finlayson, K.; Turnbull, L.; January, C. T.; Sharkey, J.; Kelly, J. S. [^{3}H]Dofetilide binding to hERG transfected membranes: a potential high throughput preclinical screen. *Eur. J. Pharmacol.* **2001**, *430*, 147−148.
(42) Qu, Y.; Fang, M.; Gao, B.; Chui, R. W.; Vargas, H. M. BeKm-1, a Peptide Inhibitor of Human *ether-a-go-go*-Related Gene Potassium Currents, Prolongs QTc Intervals in Isolated Rabbit Heart. *J. Pharmacol. Exp. Ther.* **2011**, *337*, 2−8.
(43) Patel, S.; Vuillard, L.; Cleasby, A.; Murray, C. M.; Yon, J. Apo and Inhibitor Complex Structures of BACE (b-secretase). *J. Mol. Biol.* **2004**, *343*, 407−416.
(44) Otwinowski, Z.; Minor, W. Processing of X-ray diffraction data collected in oscillation mode. *Methods Enzymol.* **1997**, *276*, 307−326.
(45) Murshudov, G. N.; Vagin, A. A.; Dodson, E. J. Refinement of macromolecular structures by the maximum-likelihood method. *Acta Crystallogr., Sect. D: Biol. Crystallogr.* **1997**, *D53*, 240−255.
(46) Emsley, P.; Cowtan, K. Coot: model-building tools for molecular graphics. *Acta Crystallogr., Sect. D: Biol. Crystallogr.* **2004**, *D60*, 2126−2132.